Supplemental Information for: "De novo 3D models of SARS-CoV-2 RNA elements from consensus experimental secondary structures"

Ramya Rangan[1*], Andrew M. Watkins[2*], Jose Chacon[2], Rachael Kretsch[1], Wipapat Kladwang[2], Ivan N. Zheludev[2], Jill Townley[3], Mats Rynge[4], Gregory Thain[5], Rhiju Das[1,2,6†]

[1] Biophysics Program, Stanford University, Stanford CA 94305
[2] Department of Biochemistry, Stanford University School of Medicine, Stanford CA 94305
[3] Eterna Massive Open Laboratory
[4] Information Sciences Institute, University of Southern California, Marina Del Rey, CA 90292, USA
[5] Department of Computer Sciences, University of Wisconsin–Madison, Madison, WI 53706 USA
[6] Department of Physics, Stanford University, Stanford CA 94305

* Equally contributing lead authors.
† Corresponding author: rhiju@stanford.edu

This supplemental information contains 8 Supplementary Figures and 4 Supplementary Tables.

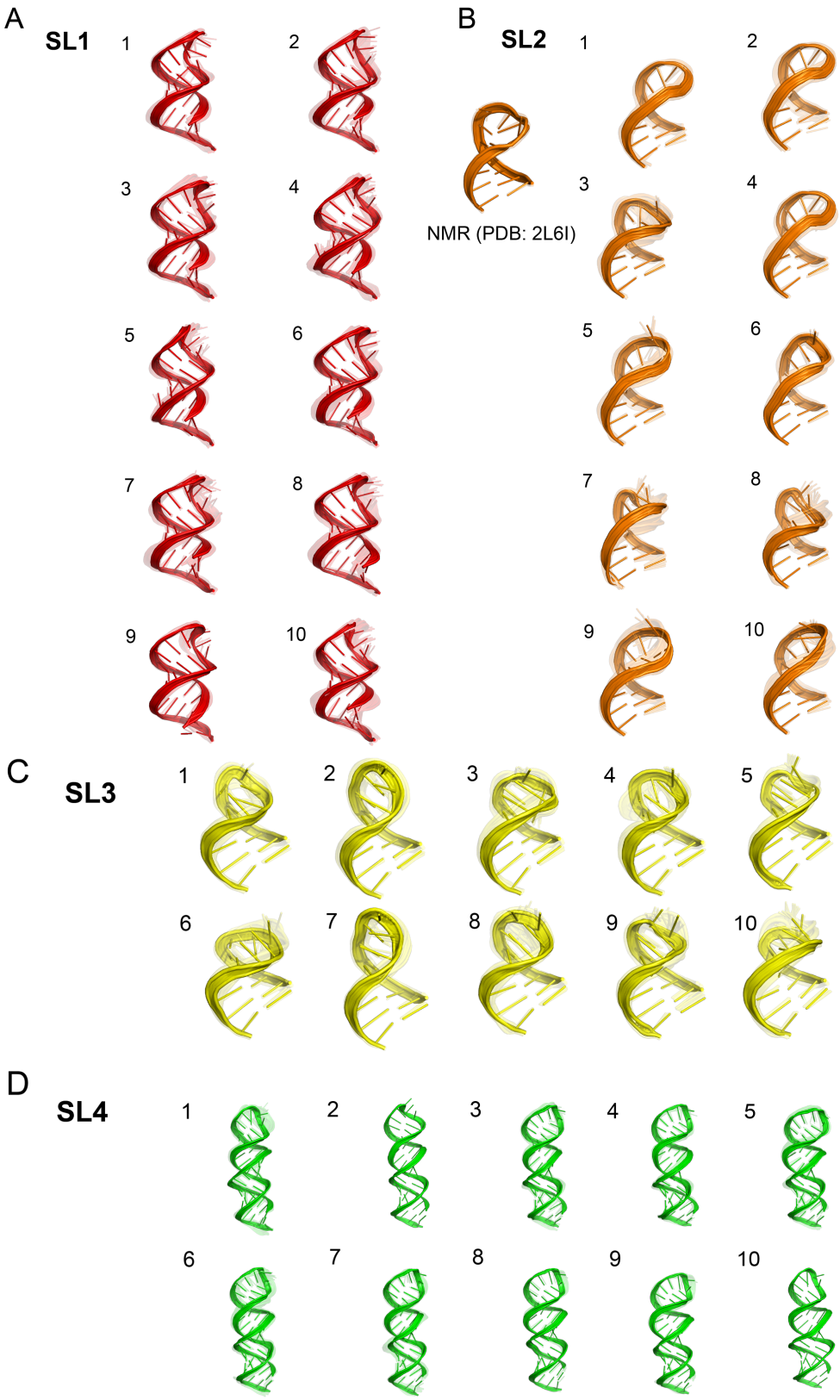
A
SL1
1
2
3
4
5
6
7
8
9
10
B
SL2
NMR (PDB: 2L6I)
1
2
3
4
5
6
7
8
9
10
C
SL3
1
2
3
4
5
6
7
8
9
10
D
SL4
1
2
3
4
5
6
7
8
9
10

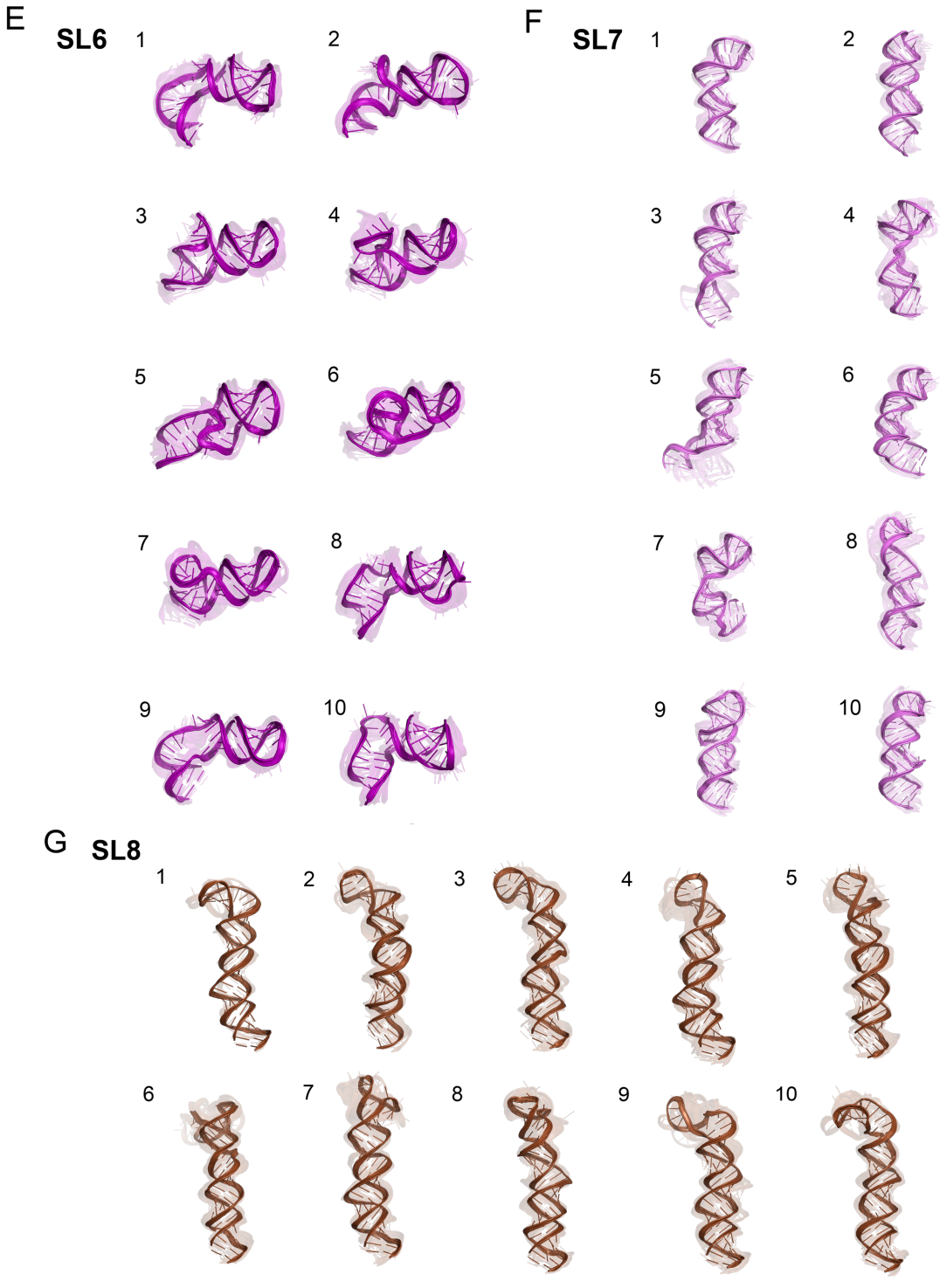
E
SL6
1
2
3
4
5
6
7
8
9
10
F
SL7
1
2
3
4
5
6
7
8
9
10
G
SL8
1
2
3
4
5
6
7
8
9
10

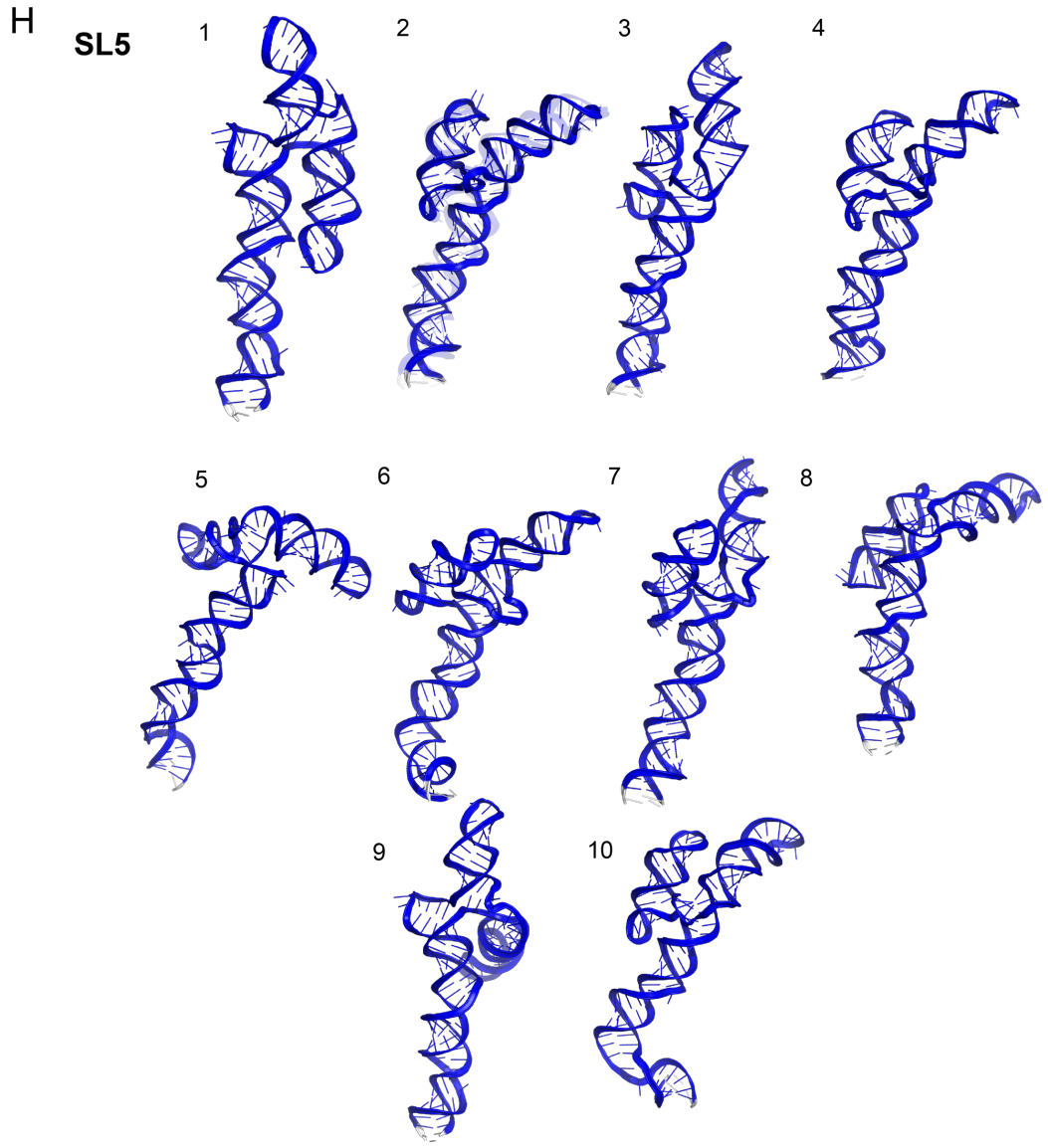

Supplementary Figure 1. *Models for the extended 5′ UTR.* Top 10 clusters are depicted for segments of the extended 5′ UTR: A) SL1, B) SL2, C) SL3, D) SL4, E) SL6, F) SL7, G) SL8, and H) SL5. Models are colored analogously to the secondary structure in Fig. 1.

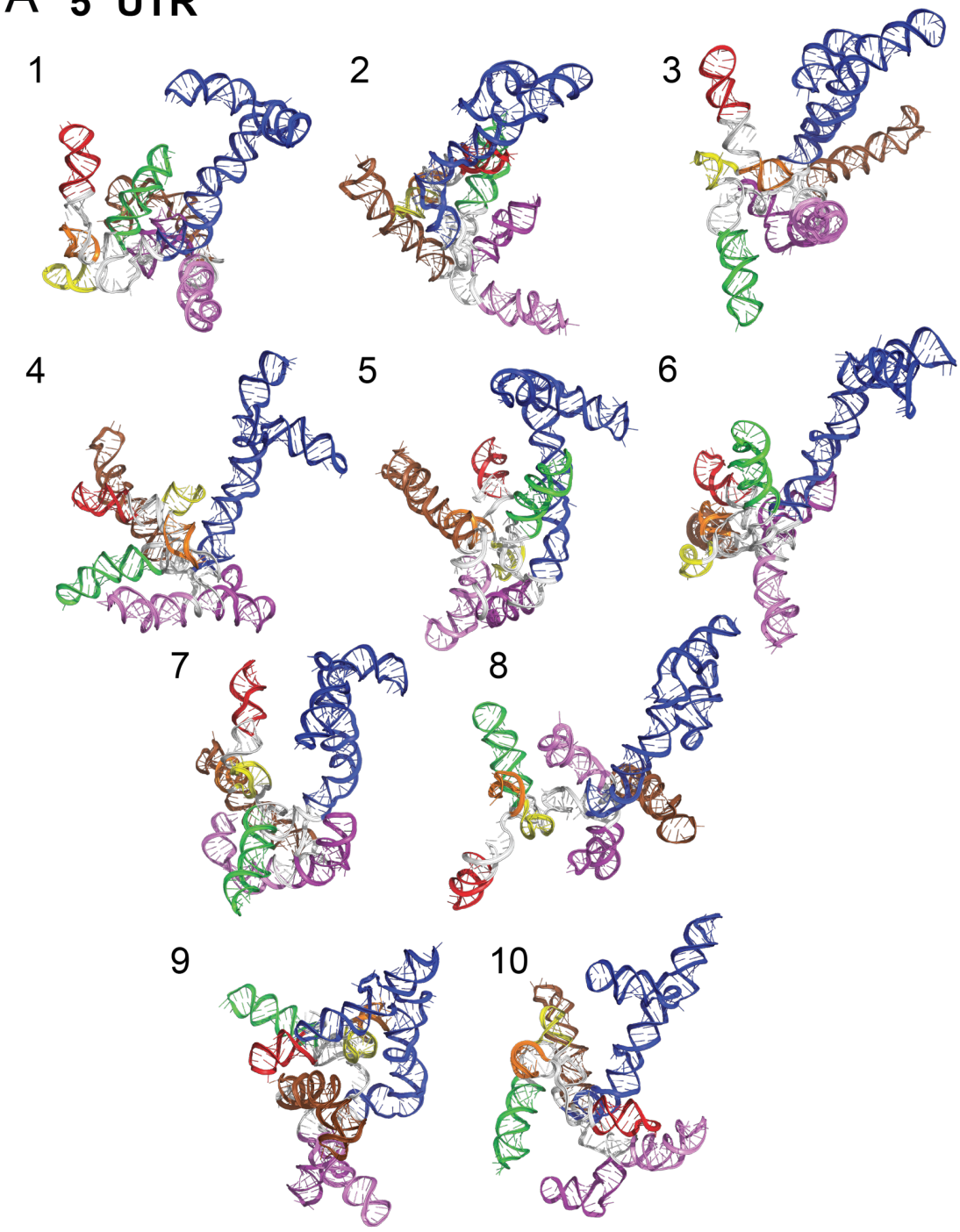
A
5′ UTR
1
2
3
4
5
6
7
8
9
10

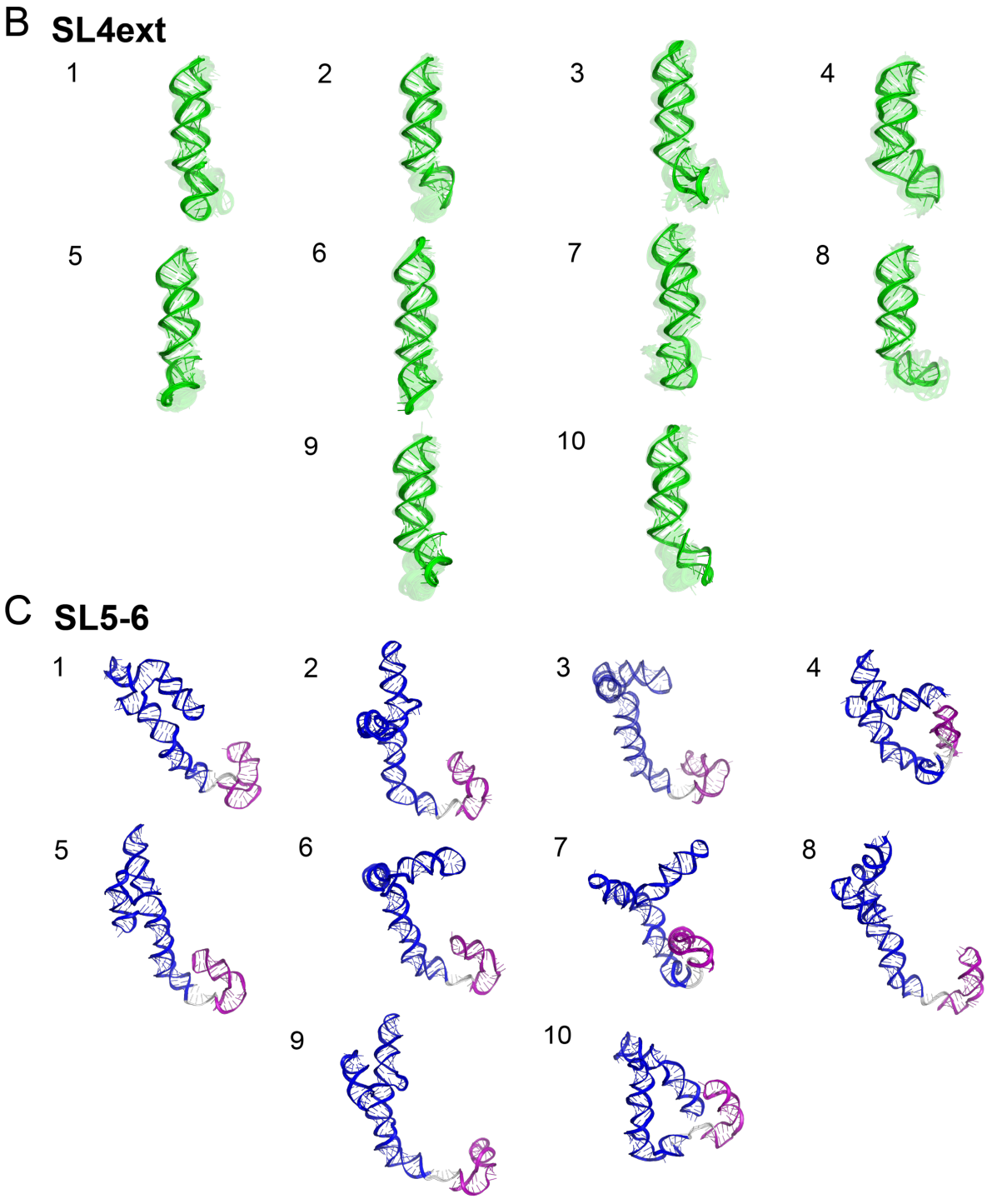

Supplementary Figure 2. *Models for the extended 5′ UTR, single occupancy clusters.* A) Top 10 clusters (all single-occupancy) are depicted for the extended 5′ UTR, colored analogously to the secondary structure in Fig. 1. B) Top 10 clusters for SL4 in the 5′ UTR along with a helix at the 3′ end predicted from some chemical mapping studies. C) Top 10 clusters for the SL5-6 in the 5′ UTR.

A

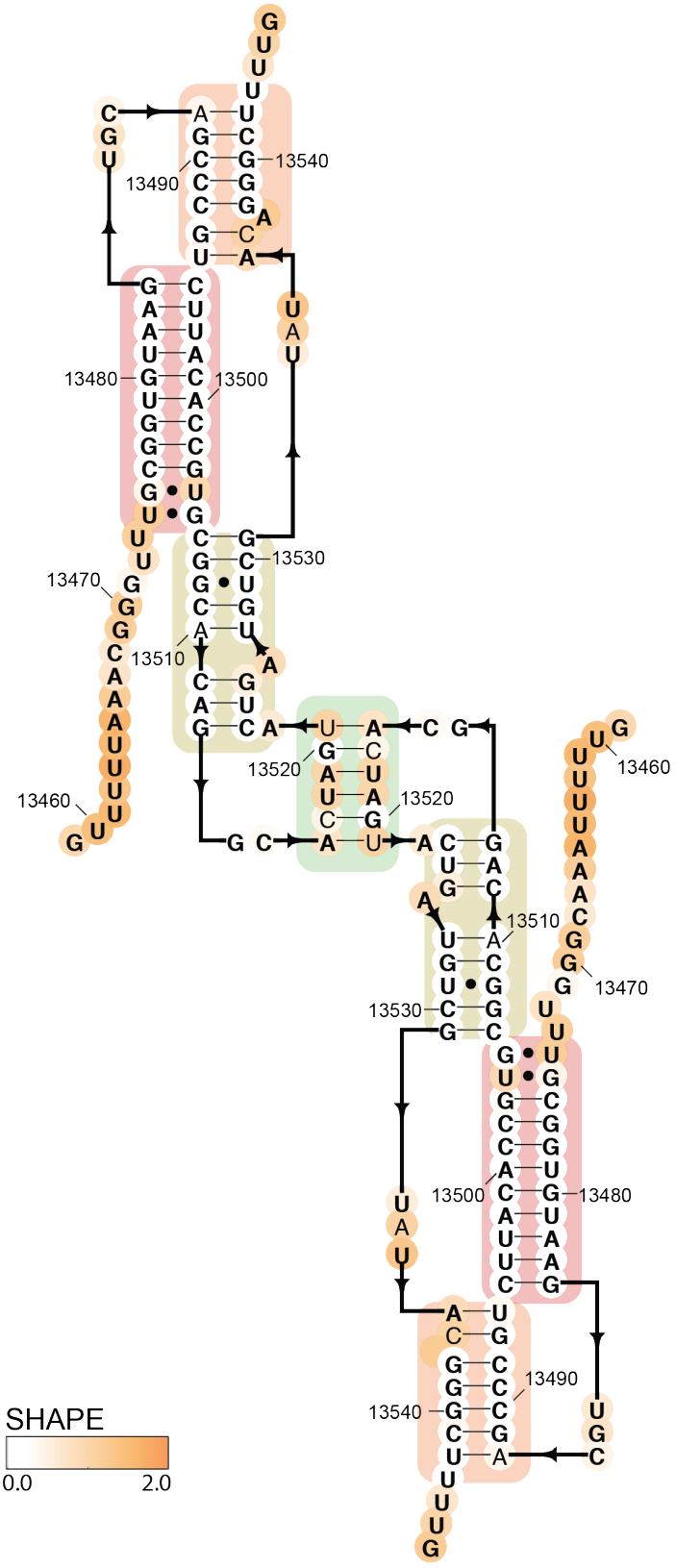
13490
13540
13480
13500
13530
13470
13510
13460
13520
13510
13470
13460
13530
13500
13480
13490
13540
SHAPE
0.0
2.0

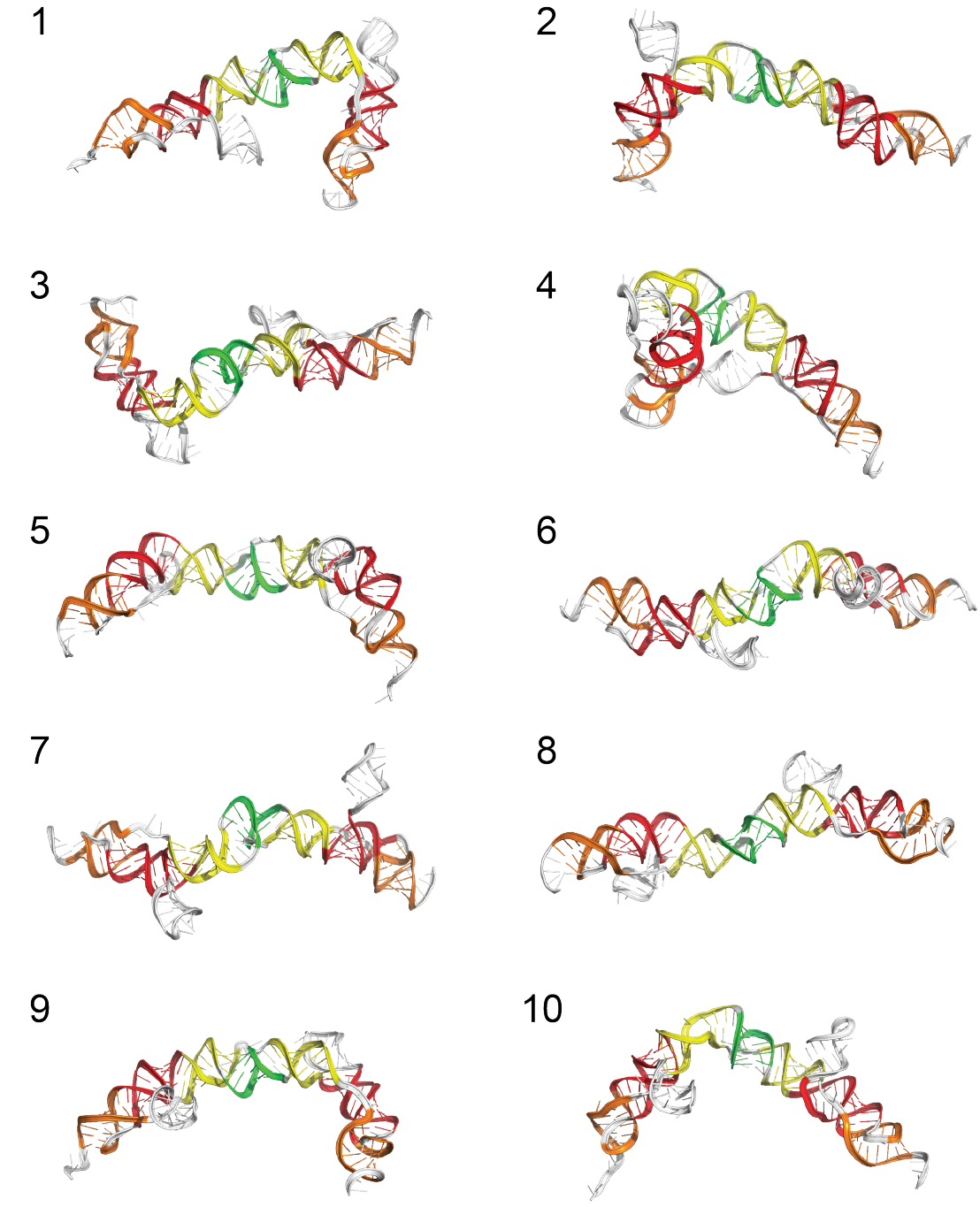

Supplementary Figure 3. *Models for the putative frameshift stimulation element dimer*. A) Secondary structure for the FSE dimer, generated from the secondary structure of the FSE in Fig. 3. B) Top 10 clusters (all single-occupancy) are depicted for the frameshift stimulating element dimer, colored analogously to the secondary structure in Fig. 3.

A

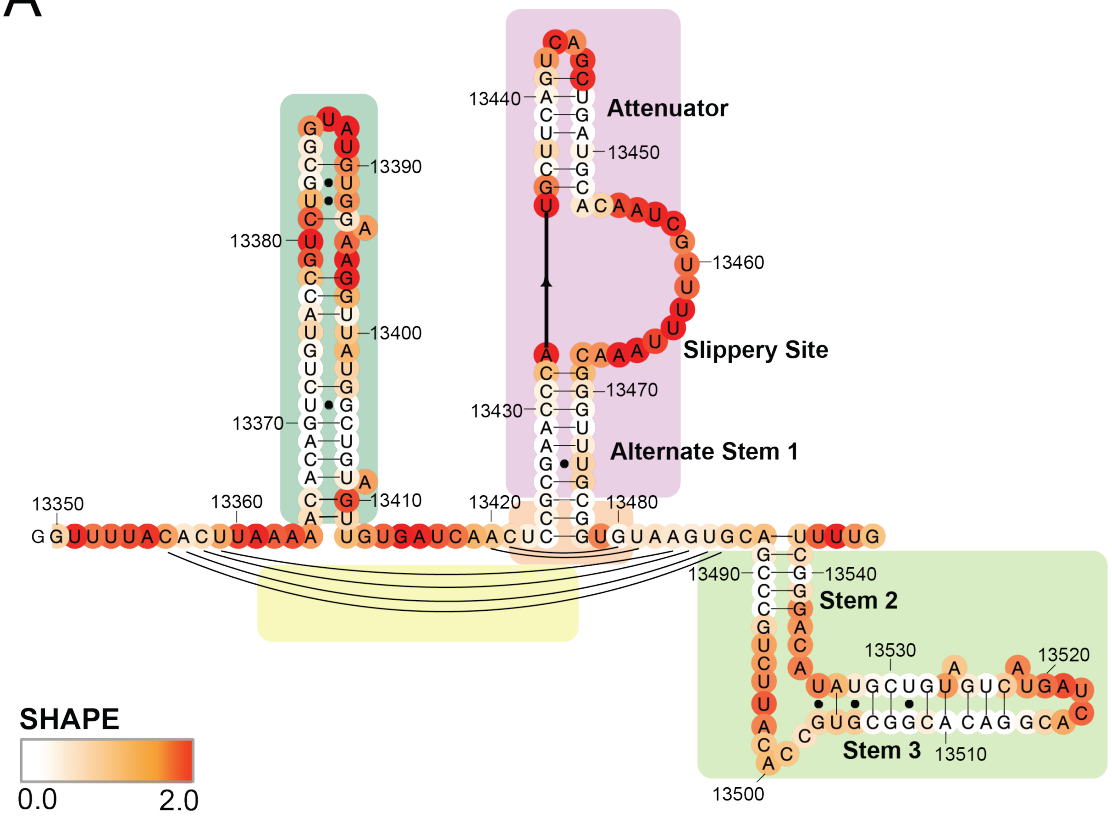
Attenuator
Slippery Site
Alternate Stem 1
Stem 2
Stem 3
13350
13360
13370
13380
13390
13400
13410
13420
13430
13440
13450
13460
13470
13480
13490
13500
13510
13520
13530
13540
SHAPE
0.0
2.0

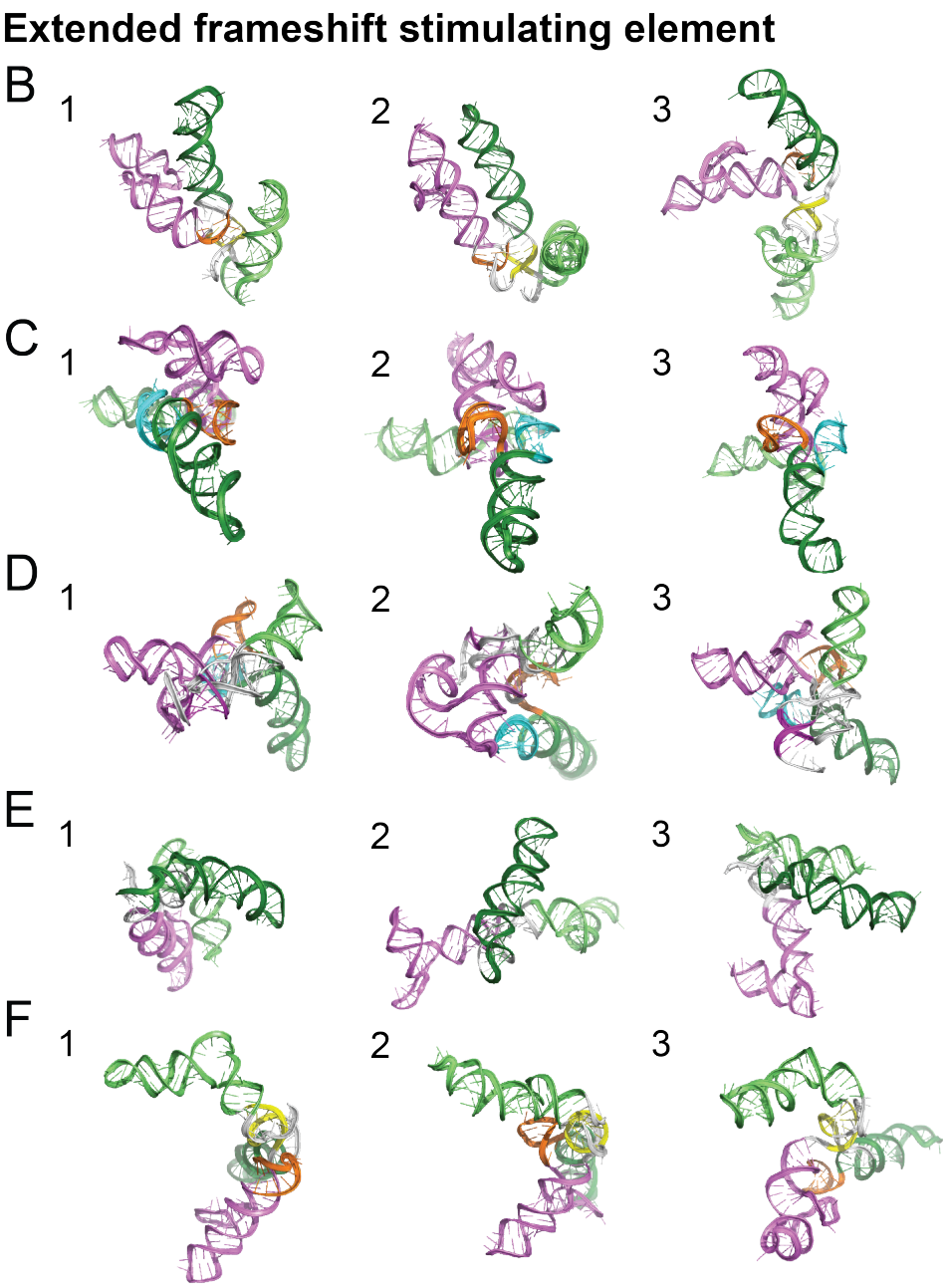

Supplementary Figure 4. *Models for the extended frameshift stimulation element with different secondary structures*. A) Secondary structure for the extended FSE as predicted from RNAstructure guided by the SHAPE data collected Zhang, et al.[1] for this extended FSE construct. Top 3 clusters are depicted for an extended segment including the frameshift stimulating element using secondary structures predicted by RNAstructure guided by chemical reactivity data from B) Zhang, et al.[1] C) Manfredonia, et al.[2] D) Huston, et al.[3] E) Lan, et al.[4] and F) Iserman, et al.[5]

A 3´ UTR

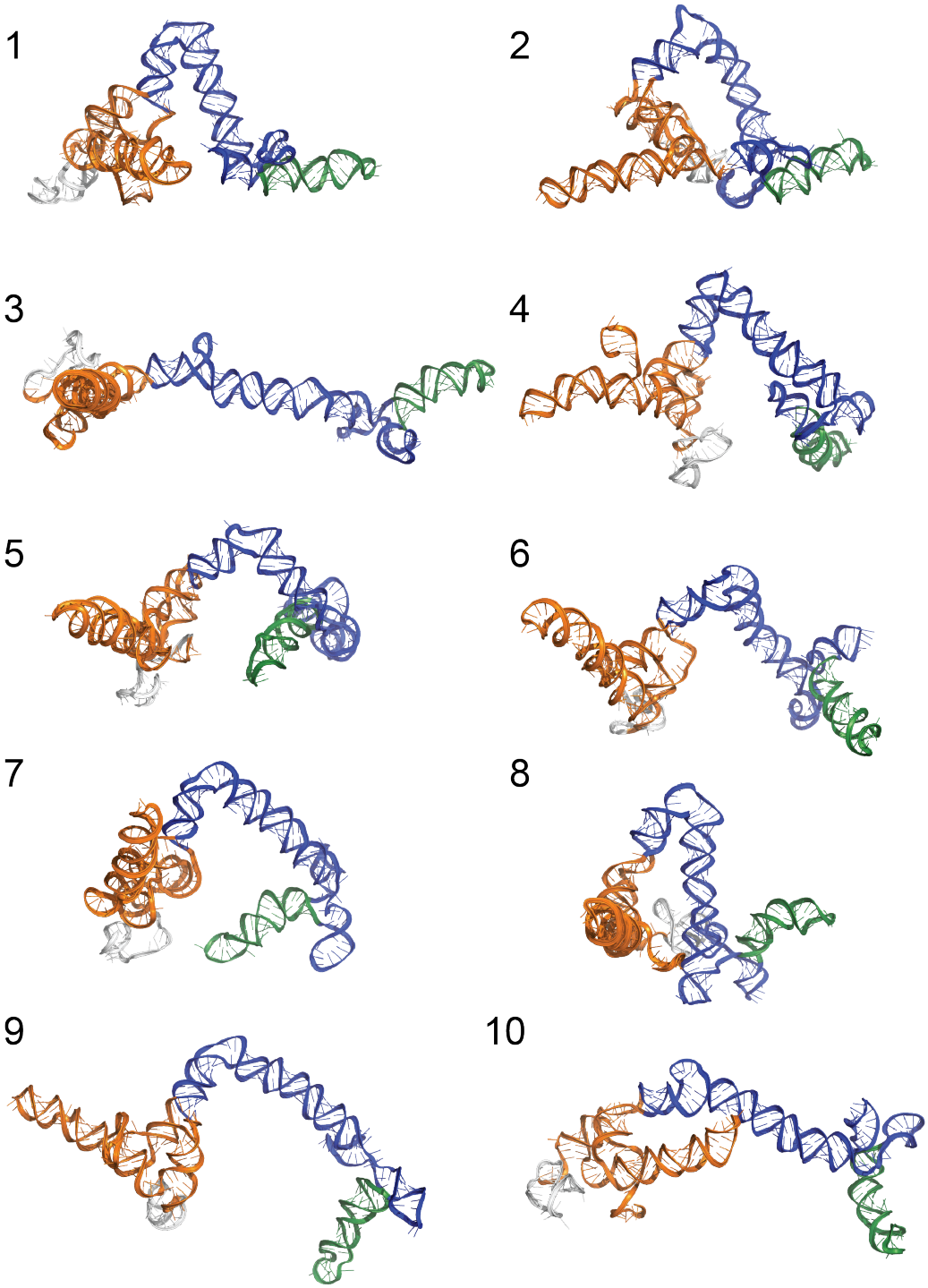

B **Extended 3´ UTR Pseudoknot**

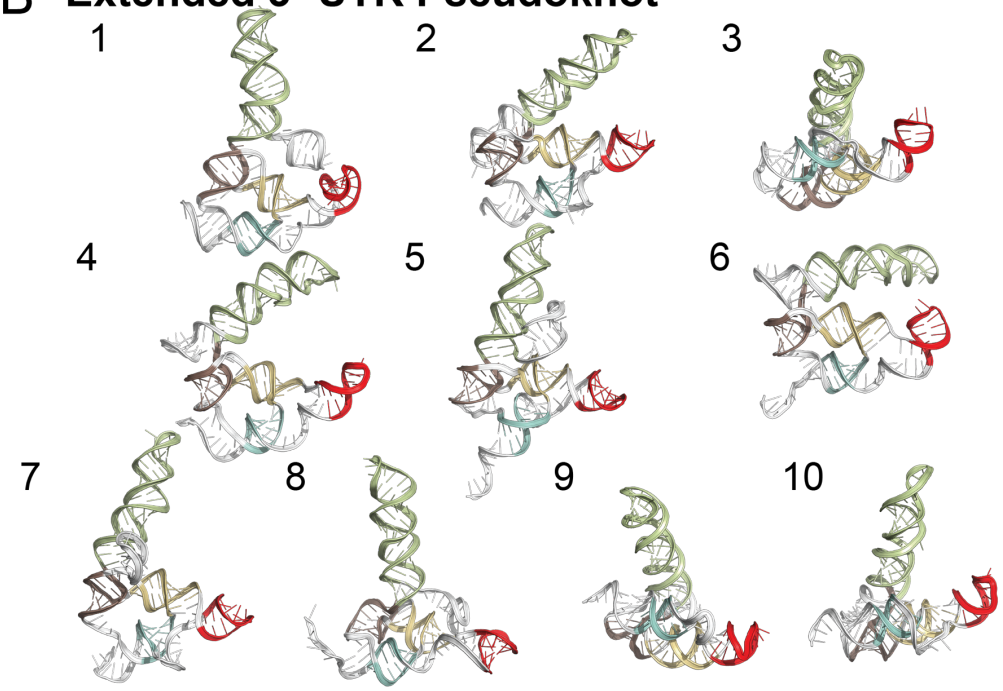

C **3´ UTR Extended BSL**

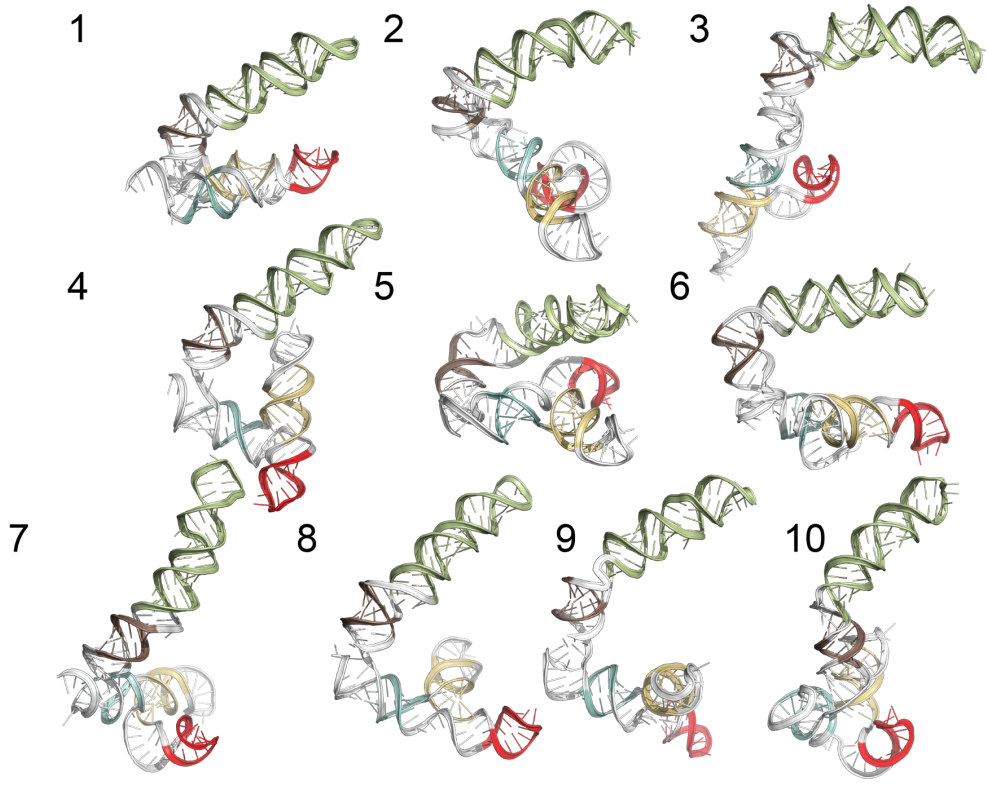

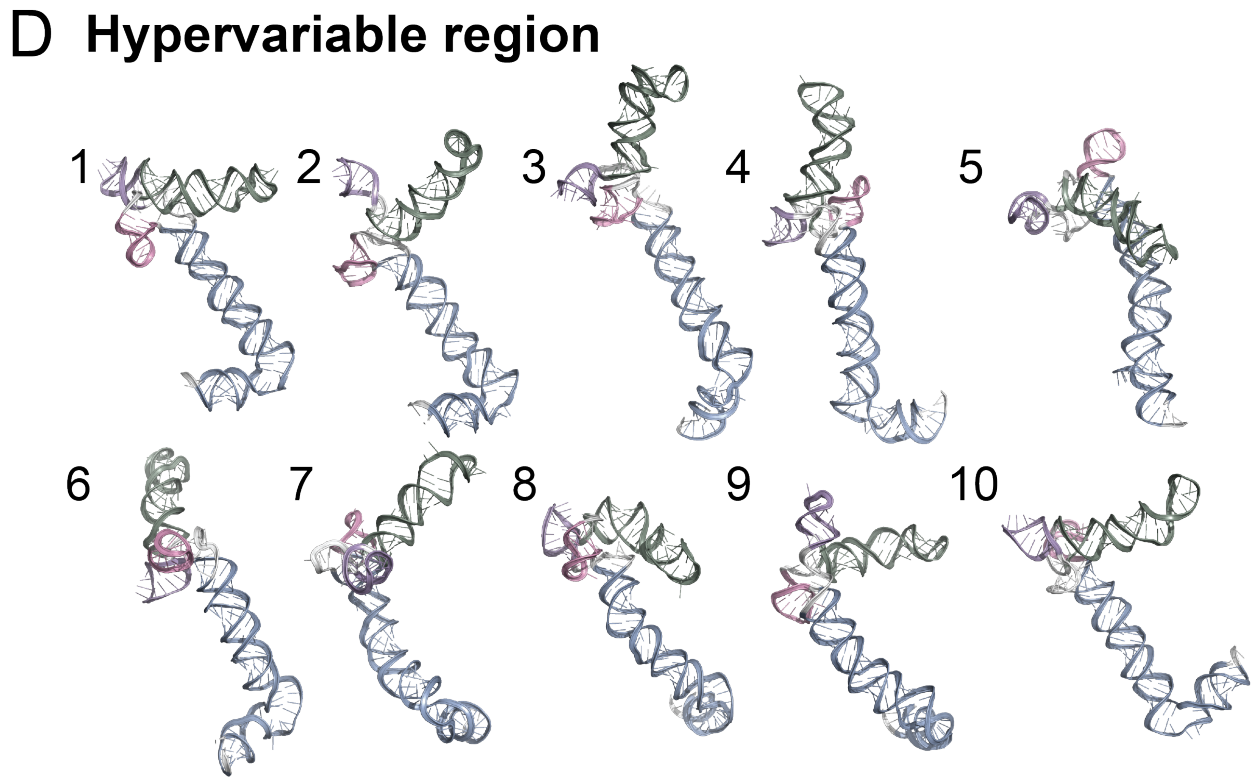

Supplementary Figure 5. *Models for full 3′ UTR and segments of the 3′ UTR*. Top 10 clusters (all single-occupancy) are depicted for the A) complete 3′ UTR, B) 3′ UTR pseudoknot, C) 3′ UTR extended BSL, and D) hypervariable region. Structures are colored analogously to the 3′ UTR secondary structure in Fig. 4.

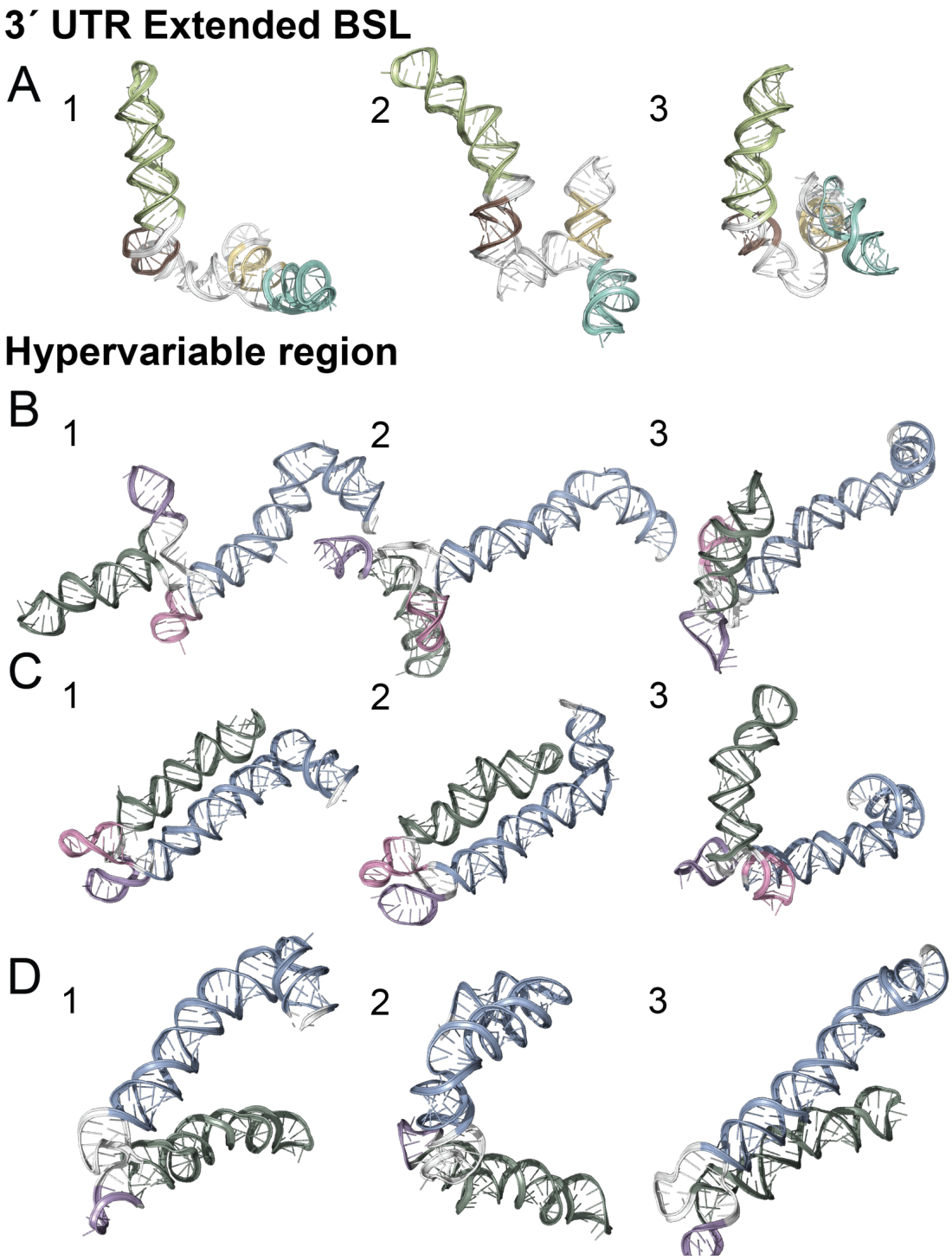

Supplementary Figure 6. *Models for segments of the 3′ UTR with alternate secondary structures.* A) Top 3 clusters are depicted for the 3′ UTR pseudoknot / extended BSL region with secondary structure as predicted from RNAstructure guided by chemical reactivity data from Huston, et al.[3] Top 3 clusters are depicted for the hypervariable region with structures predicted from RNAstructure guided by chemical reactivity data from B) this study (see Methods), C) Manfredonia, et al.[2], and D) Huston, et al.[3] Coloring of stems matches Fig. 4.

HOMOLOGY

A

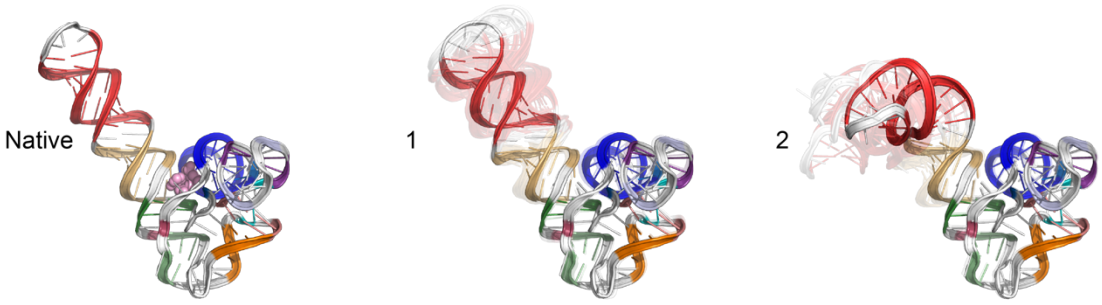

SAM-I riboswitch (RNA-Puzzle 4)

B

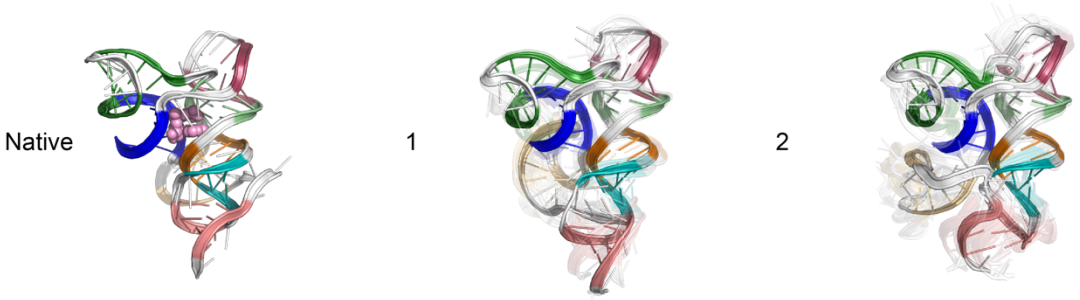

SAM-I/IV riboswitch (RNA-Puzzle 8)

C

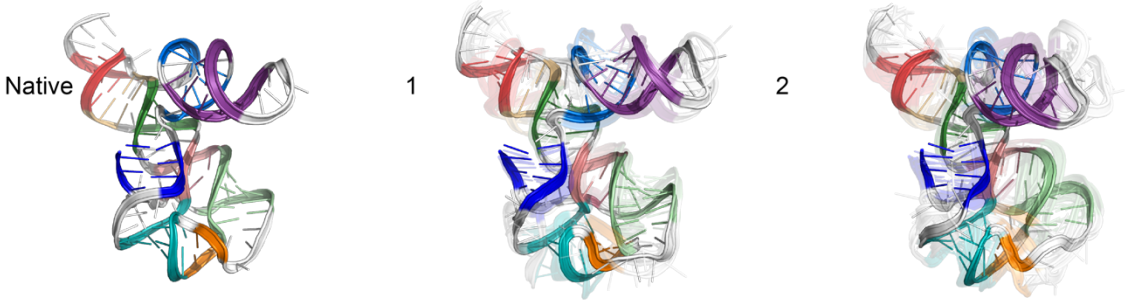

SAM-IV riboswitch (RNA-Puzzle Unknown RFam 15)

DE NOVO

D

Native

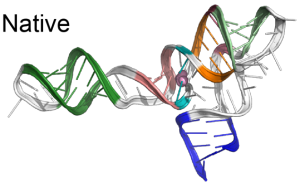

1

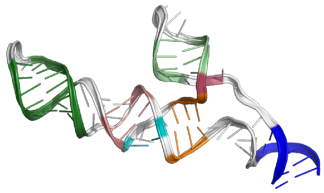

2

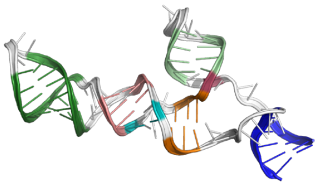

Glycine riboswitch (RNA-Puzzle 3)

E

Native

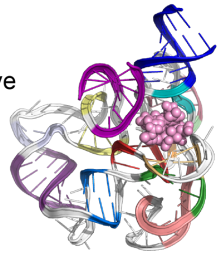

1

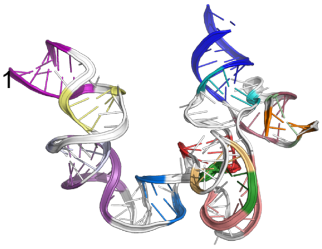

2

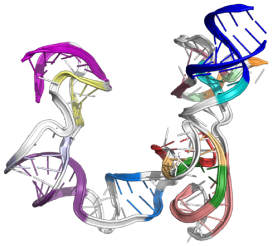

Cobalamin riboswitch (RNA-Puzzle 6)

F

Native

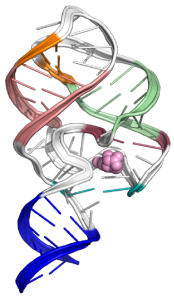

1

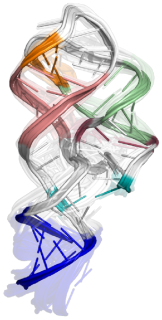

2

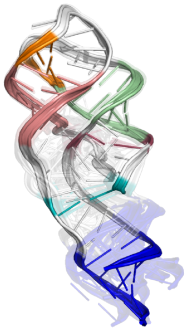

5HT aptamer (RNA-Puzzle 9)

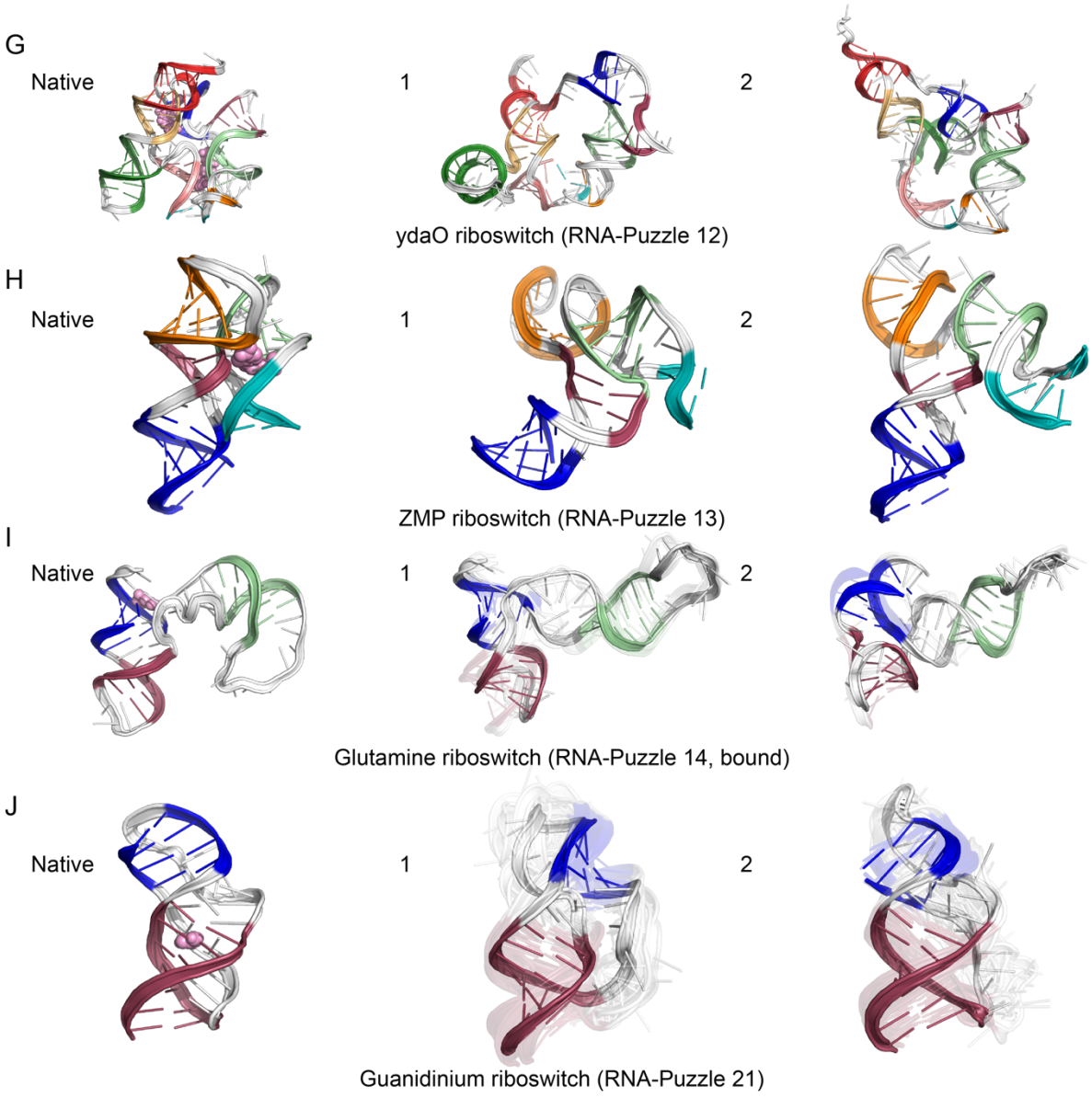

Supplementary Figure 7. Top two clusters for the following small-molecule binding RNA riboswitches and aptamers, along with their native structure (left in each panel, with ligand in pink spheres), beginning with three template-guided modeling challenges: A) SAM-I riboswitch, B) SAM-I/IV riboswitch, C) SAM-IV riboswitch, D) glycine riboswitch, E) cobalamin riboswitch, F) 5HT riboswitch, G) cyclic diGMP ydaO riboswitch , H) ZMP riboswitch, I) glutamine riboswitch, J) guanidinium riboswitch. The top-scoring cluster member in each case is depicted with solid colors, and the top cluster members (up to 10) are depicted as transparent structures.

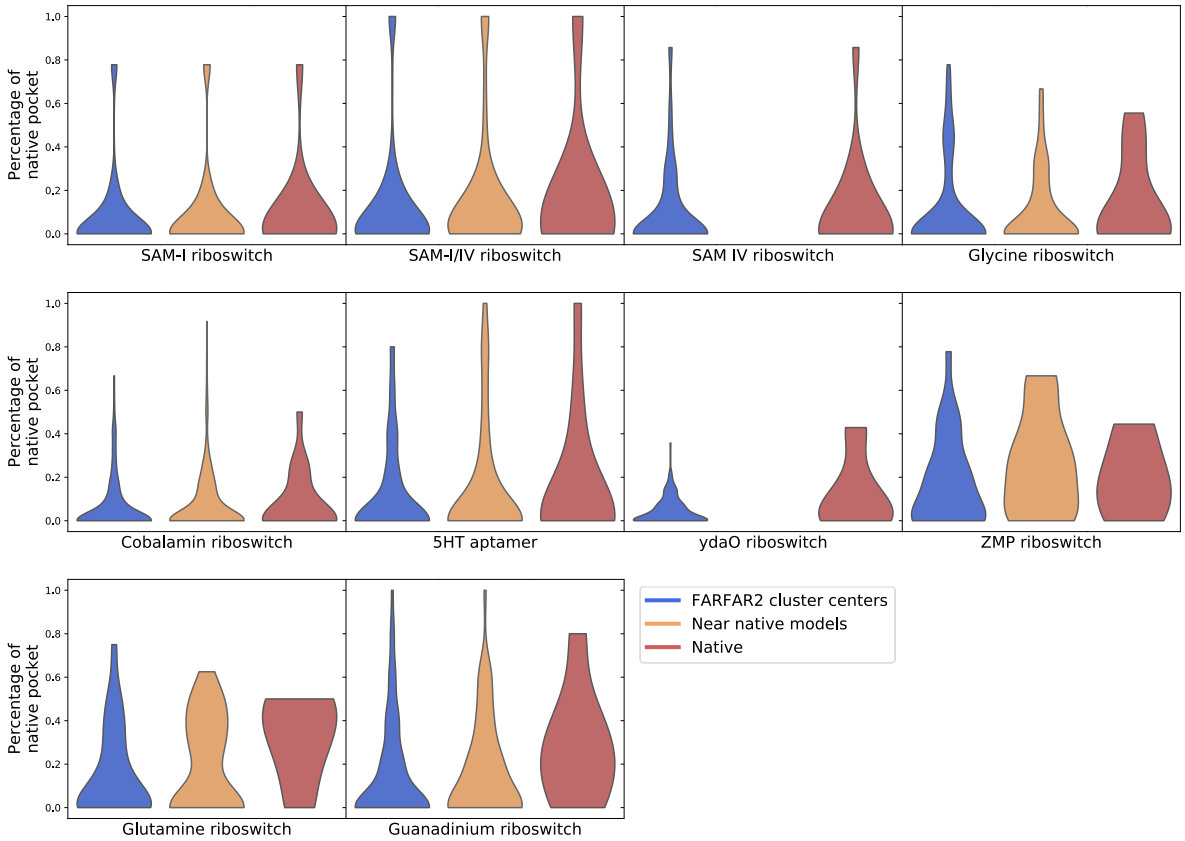

Supplementary Figure 8. Percent of native pocket residues included in pocket predictions for ten small-molecule binding RNA riboswitches and aptamers. For each of these 10 cases, pockets were predicted with fpocket for the native structure with the ligand removed, for models constrained to be near-native, and for FARFAR2 cluster centers. These violin plots indicate the percentage of native pocket residues recovered by predicted pockets, showing the distribution across all predicted pockets for each case.

Table S1. Secondary structures for SARS-CoV-2 genome elements.

Region	Positions	Dataset[a]	ShapeKnots vs Fold[b]	Used for 3D models	Secondary structure
5'UTR extended	1-480	Literature[6]	--	Yes	......(((((.(((((....)))))..))))).........(((((.....))))).((((.......)))). .......((((((((.((.((((.(((.....))).)))))).)))))))).....................(((((((((((..(((((...(((.((((((((((((.((((((.(((((......)))))..)))))))).....)))((((((((.((......)))))))))(((....)))))))))))))).))))).))))...)))))).... ...((((((.......((..((((((...))))))..))))))))......(((((.((((((((((((.....)))).))))..))))).))))).........((((((((.((.((((......(((((((....(((.....))))))))))....)))).)).))).)))))..
5'UTR extended	1-480	Manfredonia, et al.[2]	Fold	No	......(((((.(((((....)))))..))))).........(((((.....))))).((((.......)))). .......((((((((.((.((((.(((.....))).)))))).)))))))).....................(((((((((((..(((((...(((.(((((((((((..((((((..((((......))))...)))))).......)))((((((((.((......)))))))))(((....)))))))))))))).))))).))))...)))))))..... ..((((((.......((..((((((...))))))..))))))))...(((((((.((((((((((((.....)))).)))..)))))).)))))..)).......((((((((.((.((((..((..(((((((....(((.....))))))))))..)))))).)).)))).))))..
5'UTR extended	1-480	Huston, et al.[3]	Fold	Yes: SL8	.((((.(((((.(((((....)))))..))))).........(((((.....))))).((((.......)))) .)))).((((((((((.((.((((.(((.....))).)))))).)))))))).)).......((........)) ((((((((((..(((((...(((.(((((((((((..((((((.(((((......)))))..)))))).......)))((((((((.((......)))))))))(((....)))))))))))))).))))).))))...)))))).... ....((((((...........((((((...))))))....))))))......(((((.((((((((((((.....)))).))))..))))).)))))...........((((((((....((((..((..((((((....((((.....))))))))))..))))))....)))).))))..
5'UTR extended	1-480	Iserman, et al.[5]	Fold	No	......(((((.(((((....)))))..))))).........(((((.....))))).((((.......)))). .......((((((((.((.((((.(((.....))).)))))).)))))))).....................(((((((((((..(((((...(((.(((((((((((..((((((.(((((......)))))..)))))).......)))((((((((.((......)))))))))(((....)))))))))))))).))))).))))...)))))))..... ..((((((.......((..((((((...))))))..))))))))......(((((.((((((((((((.....)))).))))..))))).)))))...........((((((((.((.((((..((..((((((....(((((...)))))))))))..)))))).)).))).)))))..
5'UTR extended	1-480	Sun et al.[7], *in vivo*	Fold	No	.((((.(((((.(((((....)))))..))))).........(((((.....))))).((((.......)))) ......((((((((((.((.((((.(((.....))).)))))).)))))))).)).((((.....))))...... (((((((((((..(((((...(((.(((((((((((..((((((.(((((......)))))..)))))).... ..)))((((((((.((......)))))))))(((....)))))))))))))).))))).))))...))))))). ....(.((((((.......((..((((((...))))))..))))))))...).(((((.((((((((((((.. ...)))).))))..))))).)))))......)))).((((((((.((.((((..((..((((((....(((((...)))))))))))..)))))).)).)))).))))..
5'UTR extended	1-480	Sun et al.[7], *in vitro*	Fold	Yes: SL8	.((((.(((((.(((((....)))))..))))).........(((((.....))))).((((.......)))) ........((((((((.((.((((.(((.....))).)))))).))))))))((((((((.....))))))).)) (((((((((((..(((((...(((.(((((((((((..((((((.(((((......)))))..)))))).... ..)))((((((((.((......)))))))))(((....)))))))))))))).))))).))))...))))))). ......((((((.......((..((((((...))))))..))))))))...(((((((.((((((((((((.. ...)))).))))..))))).)))))..))...)))).((((((((.((.((((..((..(((((((....((((...)))))))))))..)))))).)).))).)))))..
5'UTR SL1-4	1-149	This study	Fold	Yes: extended SL4	......(((((.(((((....)))))..))))).........(((((.....))))).((((.......)))). .......((((((((.((.((((.(((.....))).)))))).))))))))((((((((.....))))))).))
5'UTR SL2-6	45-344	This study	Fold	No	(((((.....))))).......................((((((((.((.((((.(((.....))).)))))).)))))))).....................(((((((((((..(((((...(((.(((((((.(((..((((((.(((((......)))))..))))))......)))((((((((.((......)))))))))(((....))).)))))))))).))))).))))...)))))))).......((((((.......((..((((((...))))))..)))))))) .
RC_TRS	149-1	This study	Fold	Yes	..((((((((.....))))))).(((((((..(.....)..)))))))(((.((((((((((.((.((((((... ((((.......)))).(((((.....))))).)))))).))))))).))))).)))((((((....)))))).. .
plusFSE	13349-13546	Manfredonia, et al.[2]	ShapeKnots	Yes	.(((((......)))).)((((((...(((.(((((.....)))).).)))...))))))(((((....))))) ((((((((((.(((.((((....)))).)))..............))))))))))[[[[[[...((((((([]]]]]..((((((((((((....)).))).)))))))))).)))))....
plusFSE	13349-13546	Iserman, et al.[5]	Fold	Yes	.......((((((.....((((((...(((.(((((.....)))))..)))...))))))(((((....)))))(((((((((((.(((.((((....)))).)))..............))))))))))..)))))).(((((..........((((((((((... ......))).)))))))) ...)))))....
plusFSE	13349-13546	Lan, et al.[4]	Fold	Yes	.......(((.....((((((((((...(((.(((((.....)))))..)))...)))))).))))))).....(.(((((((((((.(((.((((....)))).)))..............))))))))).).......((((..........((((((((((((.. ..)).))).)))))))) ...)))).....

plusFSE	13349-13546	Huston, et al.[3]	ShapeKnots	Yes	.(((((.......)))))((((((...(((.(((((.....)))))..)))...))))))(((((....)))))...(((((((.(((.((((....)))).)))..............)))))))((((((((...[[[[[..)))))))))((((((((((.........))).)))))))....]]]]]....
plusFSE	13349-13546	Sun et al.[7], *in vivo*	Fold	Yes	((((...((((((.....((((((((.(((.((((((...))))))..))))).))))))(((((....)))))((((((((((.(((.((((....)))).))).....(((....))))))))))))..)))))).)))).(((((.....((((((((((((((....)).))).))))))))..)))))).....
plusFSE	13349-13546	Sun et al.[7], *in vitro*	ShapeKnots	Yes	(((....((((((.....((((((...(((.((((((...))))))..)))...))))))(((((....)))))((((((((((.(((.((((....)))).))).....(((....))))))))))))..)))))).[[[[[[[.....)))((((((((((((((....)).))).))))))))]].]]]]]....
plusFSE	13349-13546	Zhang et al.[1]	Fold	Yes	.....((((.....((((((((...(((..(.((.....)).)...)))...)))))).)).(.....).((.((((((((((..((.((((....)))).)).(.....).........)))))))))).)).)))).(((((..........(((((((((((.... .....))).))))))))...)))))....
FSE	13459-13546	Literature[8]	--	Yes	................((((((((((...[[[[[[[))))))))))((((((((((.........))).))))))..]].]]]]]....
FSE	13459-13546	Literatre[6]	--	Yes	...............(((((((((((...[[[[[[[)))))))))))((((((((.........))).)))))...]].]]]]]....
Pkfull	29543–29665; 29846–29876	Literature[6] (pseudoknot)	--	Yes	................((((((((((..(((...((......))...))).)))))))))))..(((((((.......{{{{{{.[[[[[[[[[.))))))))...]]]]]]]]]...((((......))))...........}}}}}}.........
Pkfull	29543–29665; 29846–29876	Literature[6] (BSL ext)	--	Yes	.....((((((.....((((((((((((..(((...((......))...))).)))))))))))..))))))........{{{{{{.((((((((((...........))))))))))...((((......))))...........}}}}}}.........
Pkfull	29543–29665; 29846–29876	Manfredonia, et al.[2]	Fold	No	.....((((((..((.(((((((((((..(((...((......))...))).))))))))))))))))))).........((((((.(((((((((.((....))..))))))))).((((((......)))).))........))))))..........
Pkfull	29543–29665; 29846–29876	Manfredonia, et al.[2]	ShapeKnots	No	.....((((((..((.(((((((((((..(((...((......))...))).))))))))))))))))))).........((((((.(((((((((.((....))..))))))))).((((((......)))).))........))))))..........
Pkfull	29543–29665; 29846–29876	Huston, et al.[3]	Fold	No	.....((((((..((.(((((((((((..(((...((......))...))).))))))))))))))))))).((........))..((((((((((...........)))))))))).((((((.(((.((....)).))))))).))..............
Pkfull	29543–29665; 29846–29876	Huston, et al.[3]	ShapeKnots	Yes	.....((((((..((.(((((((((((..(((...((......))...))).))))))))))))))))))).............((((((((((...........)))))))))).((((((.(((..........))))))).))...........
Pkfull	29543–29665; 29846–29876	Sun et al.[7], *in vivo*	Fold	No	.....(((((((..(.(((((((((((..(((...((......))...))).))))))))))))))))))).........((((((.(((((((((.((....))..))))))))).((((((......)))).))((....))))))))..........
Pkfull	29543–29665; 29846–29876	Sun et al.[7], *in vivo*	ShapeKnots	No	.....(((((((..(.(((((((((((..(((...((......))...))).))))))))))))))))))).........((((((.(((((((((.((....))..))))))))).((((((......)))).))((....))))))))..........
Pkfull	29543–29665; 29846–29876	Sun et al.[7], *in vitro*	Fold	No	.....(((((((..(.(((((((((((..(((...((......))...))).))))))))))))))))))).........((((((.(((((((((.((....))..))))))))).((((((......)))).))((....))))))))..........
Pkfull	29543–29665; 29846–29876	Sun et al.[7], *in vivo*	ShapeKnots	No	.....(((((((..(.(((((((((((..(((...((......))...))).))))))))))))))))))).........((((((.(((((((((.((....))..))))))))).((((((......)))).))((....))))))))..........
HVR	29659–29852	Literature[6]	--	Yes	..((((..((((((((((..((..(((.(((.....((((((((.((.(((....)))))....((((((((....((..((((.....))..))...))...))))).)))).((((........))))..........))))))))).....))).)))..))...)))))......)))))..))))..
HVR	29659–29852	Manfredonia, et al.[2]	Fold	Yes	..((((..((((((((((..((..(((.(((.....((((((((.((.(((....))))).((.(((((((((....((.((.((.(.......))).))))...))))).))))...)).....((.((.....)).))..))))))))).....))).)))..))...))))......))))))..))))..
HVR	29659–29852	Huston, et al.[3]	Fold	Yes	..((((..((((((((((..((..(((.........((((((((...........(((..((.((((((((....((.((...((......))..))))...))))).))))...))....))).((.....)).....))))))))).........)))..))...))))))......))))..))))..
HVR	29659–29852	This study	Fold	Yes	..((((..((((((((((..((..(((.(((.....((((((((.((.(((....)))))....((((((((....((.((.(((........))).))))...))))).)))).((((........))))..........))))))))).....))).)))..))...))))......))))))..))))..

HVR	29659–29852	Sun et al.[7], *in vivo*	Fold	No	..((((..((((((((((..((..(((.(((.....(((((((((.((.(((....))))).((.(((((((((....(.(((.(((.....))).))))...)))))).))))...)).....((.((.....)).).)..)))))))).....))).)))..))...))))......))))))..)))).. ..((((..((((((((((..((..(((.(((.....(((((((((.((.(((....))))).(((((((((((....(.(((.(((.....))).))))...)))))).))))..((((.....)))).)..))).....))))))))).....))).)))..))...))))......))))))..)))).....(((((((((((..(((...((.....))...))).)))))))))..(((((((.....{{{{{{.[[[[[[[[[.)))))))...]]]]]]]]]...((((..((((((((((..((..(((.(((.....(((((((((.((.(((....))))).....((((((((((....((..((((.....))..))...))...)))))).)))).((((.....)))).....)))))))))).....))).)))..))...)))))).....))))))..))))..........}}}}}}.....
s2m	29724-29773	Wacker, et al.[9]	--	Yes	(((((.....(((.((.....)).))).....)))))
s2m	29724-29773	Manfredonia, et al.[2]	Fold	Yes	(((((....((.((.((.(.....))).))))...)))))
s2m	29724-29773	This study	Fold	Yes	(((((....((.((.(((.....))).))))...)))))
s2m	29724-29773	Huston, et al.[3]	Fold	Yes	(((((....((.((...((.....))..))))...)))))

[a]Chemical probing dataset used to model secondary structure. `Literature` indicates that structure was obtained from consensus structures reported in prior research.
[b]RNAstructure predictions guided by chemical reactivity data were run with Fold (no pseudoknots allowed) or ShapeKnots (pseudoknots predicted).

Table S2. FARFAR2-SARS-CoV-2 models, extended data.

System/cluster	Length	Models generated	Model convergence (Å)[a]	Predicted Minimum RMSD (Å)[b]	E-gap to lowest energy model (REU)[c]	Cluster occupancy[d]	Number of pockets predicted[e]
Extended 5′ UTR (1–480)							
5′ UTR/1	480	66011	50.9	44.92 ± 6.13	0	1	58
5′ UTR/2					5.15	1	55
5′ UTR/3					12.45	1	55
5′ UTR/4					12.66	1	50
5′ UTR/5					12.98	1	57
5′ UTR/6					13.07	1	53
5′ UTR/7					13.92	1	57
5′ UTR/8					14.9	1	64
5′ UTR/9					15.43	1	66
5′ UTR/10					21.01	1	68
5′ UTR stem-loop 1 (7–33)							
SL1/1	27	200000	1.83	5.17 ± 0.52	0	6	1
SL1/2					0.07	16	0
SL1/3					0.26	45	0
SL1/4					0.91	13	1
SL1/5					0.97	6	2
SL1/6					1.02	18	1
SL1/7					1.04	9	0
SL1/8					1.27	14	0
SL1/9					1.55	4	3
SL1/10					1.57	12	2
5′ UTR stem-loop 2 (45–59)							
SL2/1	15	200000	2.39	5.63 ± 0.74	0	52	1
SL2/2					0.73	44	1
SL2/3					0.95	78	0

SL2/4					0.98	56	1
SL2/5					1.08	15	0
SL2/6					1.13	207	0
SL2/7					1.15	26	1
SL2/8					1.38	29	1
SL2/9					1.4	13	1
SL2/10					1.48	41	0
SL2/Homology					20.2	27	0
5′ UTR stem-loop 3 (61–75)							
SL3/1	15	200000	2.58	5.78 ± 0.70	0	7	1
SL3/2					0.1	45	1
SL3/3					0.61	10	1
SL3/4					0.78	69	0
SL3/5					1.31	70	1
SL3/6					1.55	6	1
SL3/7					1.89	84	0
SL3/8					1.93	49	1
SL3/9					2.1	35	0
SL3/10					2.23	18	1
5′ UTR stem-loop 4 (84–127)							
SL4/1	44	2018457	1.82	5.16 ± 0.49	0	5	2
SL4/2					0.05	1	0
SL4/3					0.91	4	5
SL4/4					0.95	4	2
SL4/5					1.03	5	4
SL4/6					1.16	11	2
SL4/7					1.43	6	1
SL4/8					1.74	2	1
SL4/9					1.91	3	2
SL4/10					1.92	1	1
5′ UTR stem-loop 5 (148–295)							

SL5/1	148	2392320	18.99	19.07 ± 6.15	0	1	12
SL5/2					1.39	2	22
SL5/3					1.46	1	18
SL5/4					2.31	1	21
SL5/5					2.32	1	14
SL5/6					3.1	1	13
SL5/7					3.35	1	18
SL5/8					3.87	1	18
SL5/9					4.16	1	12
SL5/10					4.23	1	20
5′ UTR stem-loop 5/6 (148–343)							
SL56/1	196	2020963	25.91	24.68 ± 6.27	0	1	19
SL56/2					4.42	1	20
SL56/3					4.89	2	21
SL56/4					5.69	1	24
SL56/5					6.75	1	25
SL56/6					8.16	1	22
SL56/7					8.21	1	23
SL56/8					8.47	1	21
SL56/9					8.52	1	23
SL56/10					8.92	1	17
5′ UTR stem-loop 6 (302–343)							
SL6/1	42	200000	8.92	10.92 ± 2.21	0	162	4
SL6/2					4.21	537	2
SL6/3					4.97	27	5
SL6/4					5.32	12	4
SL6/5					5.37	119	3
SL6/6					5.38	193	3
SL6/7					6.03	15	5
SL6/8					6.42	47	5

SL6/9					6.64	26	3
SL6/10					6.86	148	6
5′ UTR stem-loop 7 (349–394)							
SL7/1	27	200000	7.39	9.67 ± 1.90	0	256	2
SL7/2					1.35	292	2
SL7/3					12.24	726	2
SL7/4					14.6	15	3
SL7/5					17.5	46	7
SL7/6					20.22	2449	5
SL7/7					23.11	9	5
SL7/8					23.61	20	4
SL7/9					23.88	43	3
SL7/10					25.41	331	2
5′ UTR stem-loop 8 (407-478)							
SL8/1	72	4055322	6.86	9.24 ± 1.47	0	3	7
SL8/2					2.51	7	4
SL8/3					3.11	18	8
SL8/4					6.27	15	7
SL8/5					6.96	47	6
SL8/6					7.55	27	9
SL8/7					7.7	21	4
SL8/8					8.06	26	5
SL8/9					8.69	17	4
SL8/10					10.55	32	2
5′ UTR reverse complement stem-loops1-4 (149 - 1)							
RC-SL1-4/1	149	2031710	19.61	19.57 ± 4.37	0	1	14
RC-SL1-4/2					1.5	1	14
RC-SL1-4/3					3.83	1	11
RC-SL1-4/4					4.41	1	8
RC-SL1-4/5					4.5	1	13

RC-SL1-4/6					4.78	1	11
RC-SL1-4/7					4.8	1	16
RC-SL1-4/8					6.01	1	8
RC-SL1-4/9					7.78	1	7
RC-SL1-4/10					9.21	1	22
Frameshift stimulating element (13459–13546)							
FSE/1	88	390722	14.45	15.39 ± 3.09	0	5	8
FSE/2					3.23	1	9
FSE/3					4.44	2	9
FSE/4					5.44	3	11
FSE/5					6.22	2	12
FSE/6					7.47	2	10
FSE/7					7.78	1	11
FSE/8					7.81	4	7
FSE/9					8.06	11	11
FSE/10					8.17	8	14
Suspected frameshift stimulating element dimer (13459–13546 x 2)							
FSE Dimer/1	176	23066	21.99	21.50 ± 4.08	0	1	23
FSE Dimer/2					6.37	1	25
FSE Dimer/3					6.79	1	25
FSE Dimer/4					10.02	1	22
FSE Dimer/5					10.11	1	22
FSE Dimer/6					10.22	1	23
FSE Dimer/7					10.31	1	29
FSE Dimer/8					11.55	1	29
FSE Dimer/9					12.06	1	28
FSE Dimer/10					12.45	1	26
3´ UTR beginning with bulged hairpin (29511-29871)							
3′ UTR/1	361	11430	39.71	35.85 ± 5.51	0	1	50
3′ UTR/2					4.07	1	62

3′ UTR/3					26.33	1	47
3′ UTR/4					32.67	1	54
3′ UTR/5					42.1	1	55
3′ UTR/6					43.14	1	59
3′ UTR/7					46.96	1	46
3′ UTR/8					47.55	1	54
3′ UTR/9					48.04	1	49
3′ UTR/10					48.28	1	43
3´ UTR hypervariable region (29659-29852)							
HVR/1	194	28029	25.38	24.25 ± 4.18	0	1	30
HVR/2					2.49	1	16
HVR/3					3.6	1	24
HVR/4					4.16	1	28
HVR/5					5.81	1	18
HVR/6					6.79	1	26
HVR/7					7.63	1	23
HVR/8					7.77	1	26
HVR/9					9.06	1	25
HVR/10					11.08	1	25
3´ UTR pseudoknot (29543–29665; 29846–29876)							
Pseudoknot/1	158	1017205	21.93	21.45 ± 5.52	0	1	
Pseudoknot/2					1.42	1	17
Pseudoknot/3					2.87	1	28
Pseudoknot/4					3.94	1	16
Pseudoknot/5					3.95	1	18
Pseudoknot/6					4.06	1	25
Pseudoknot/7					4.27	1	18
Pseudoknot/8					4.97	1	20
Pseudoknot/9					5.37	1	25
Pseudoknot/10					6.15	1	19
3´ UTR pseudoknot fragment consisting of the pseudoknot (PK), P2, and P5 (29606–29665; 29842–29876)							

PK-P2-P5/1	95	1017205	10.24	11.99 ± 2.05	0	1	9
PK-P2-P5/2					0.64	2	15
PK-P2-P5/3					0.64	1	14
PK-P2-P5/4					0.69	2	12
PK-P2-P5/5					0.98	3	11
PK-P2-P5/6					1.02	5	13
PK-P2-P5/7					1.51	1	11
PK-P2-P5/8					1.53	1	16
PK-P2-P5/9					2.43	1	8
PK-P2-P5/10					2.82	3	15
3´ UTR BSL extended structure (29543–29665; 29846–29876)							
BSLext/1	158	1012716	24.04	23.16 ± 4.29	0	1	19
BSLext/2					0.48	1	14
BSLext/3					2.45	1	19
BSLext/4					6.22	1	15
BSLext/5					6.34	1	13
BSLext/6					6.38	1	22
BSLext/7					6.45	1	19
BSLext/8					6.56	1	16
BSLext/9					6.76	1	11
BSLext/10					6.84	1	16
3´ UTR stem-loop II-like motif, homology modeled from PDB ID: 1XJR[10] (29724–29773)							
S2M/1	50	200000	6.95	9.32 ± 0.09	0	199977	11
S2M/2					11.38	23	6
3´ UTR stem-loop II-like motif, secondary structure from NMR data in Wacker, et al.[9] (29724–29773)							
S2M/1	50	500000	2.97	6.10 ± 0.75	0	1	2
S2M/2					0.63	2	2
S2M/3					0.63	1	3
S2M/4					1.9	1	6
S2M/5					2.16	1	1

S2M/6					2.6	1	3
S2M/7					3.1	1	1
S2M/8					3.45	1	3
S2M/9					4.14	1	1
S2M/10					4.29	1	3

[a]Mean pairwise all-heavy-atom RMSD between 10 lowest energy cluster centers.
[b]Predicted RMSD to true structure.
[c]Rosetta all-atom free energy gap of cluster's lowest energy model compared to lowest energy model discovered in run. REU = Rosetta energy units, calibrated so that 1.0 corresponds approximately to 1 k_BT.
[d]Number of models that appear in each cluster. Clustering was carried out on top 400 models ranked by Rosetta all-atom free energy, based on 5.0 Å threshold, except for small RNAs (SL1-4, SL6-7, s2m), where 2.0 Å threshold was applied.
[e]Number of pockets predicted from fpocket for the cluster center decoy, using default settings for fpocket prediction.

Table S3. FARFAR2-SARS-CoV-2 models, extended data for alternate secondary structures.

System/cluster	Length	Models generated	Model convergence (Å)[a]	Predicted minimum RMSD (Å)[b]	E-gap to lowest energy model (REU)[c]	Cluster occupancy[d]	Number of pockets predicted[e]
5′ UTR stem-loop 4 extended (84–146)							
SL4ext/1	63	143897	7.5	9.76 ± 1.97	0	645	6
SL4ext/2					5.28	377	12
SL4ext/3					5.78	21	4
SL4ext/4					8.29	17	6
SL4ext/5					8.79	202	5
SL4ext/6					9.07	560	7
SL4ext/7					11.76	15	7
SL4ext/8					11.83	25	3
SL4ext/9					12.02	177	5
SL4ext/10					12.58	742	6
FSE extended, secondary structure from Zhang, et al.[1] (13349-13546)							
FSEext/1	198	993756	28.69	26.93 ± 4.46	0	1	24
FSEext/2					1.49	1	28
FSEext/3					2.28	1	43
FSEext/4					4.83	1	21
FSEext/5					5.91	1	31
FSEext/6					5.98	1	26
FSEext/7					6.69	1	22
FSEext/8					7.11	1	24
FSEext/9					7.88	1	33
FSEext/10					8.05	1	24
FSE extended, secondary structure from Manfredonia, et al.[2] (13349-13546)							
FSEext/1	198	1021344	24.16	23.26 ± 4.92	0	1	22
FSEext/2					3.77	1	20
FSEext/3					4.3	1	23

FSEext/4					4.76	2	25
FSEext/5					4.87	1	25
FSEext/6					5.54	1	23
FSEext/7					5.73	1	24
FSEext/8					6.24	1	25
FSEext/9					6.7	1	23
FSEext/10					7.39	1	34
FSE extended, secondary structure from Huston, et al.[3] (13349-13546)							
FSEext/1	198	252971	20.79	20.53 ± 6.00	0	1	25
FSEext/2					2.32	1	20
FSEext/3					9	1	25
FSEext/4					11.17	1	29
FSEext/5					11.93	1	26
FSEext/6					12.16	1	25
FSEext/7					12.62	1	25
FSEext/8					13.3	1	25
FSEext/9					14	1	23
FSEext/10					14.06	1	21
FSE extended, secondary structure from Lan, et al.[2] (13349-13546)							
FSEext/1	198	267963	31.76	29.42 ± 4.62	0	1	23
FSEext/2					5.1	1	26
FSEext/3					5.23	1	27
FSEext/4					8.23	1	28
FSEext/5					8.25	1	26
FSEext/6					9.59	1	21
FSEext/7					10.78	1	23
FSEext/8					11.69	1	33
FSEext/9					12.69	1	23
FSEext/10					13.24	1	22
FSE extended, secondary structure from Iserman, et al.[5] (13349-13546)							

FSEext/1	198	1013658	28.16	26.50 ± 5.21	0	1	22
FSEext/2					0.27	1	28
FSEext/3					1.78	1	24
FSEext/4					2.02	1	29
FSEext/5					2.09	1	25
FSEext/6					2.94	1	25
FSEext/7					4.73	1	25
FSEext/8					5.06	1	29
FSEext/9					5.52	1	20
FSEext/10					5.89	1	25
HVR, secondary structure based on chemical reactivity from this study (29659– 29852)							
HVRalt/1	194	1010583	28.17	26.51 ± 6.39	0	1	25
HVRalt/2					5.15	1	16
HVRalt/3					6.85	1	16
HVRalt/4					6.97	1	13
HVRalt/5					9.3	1	23
HVRalt/6					10	1	11
HVRalt/7					10.29	1	22
HVRalt/8					11.23	1	23
HVRalt/9					11.4	1	20
HVRalt/10					11.44	1	21
HVR, secondary structure from Manfredonia, et al.[2] (29659– 29852)							
HVRalt/1	194	1011993	25.11	24.03 ± 5.66	0	1	21
HVRalt/2					3.31	1	20
HVRalt/3					6.86	1	16
HVRalt/4					8.71	1	14
HVRalt/5					10.87	1	18
HVRalt/6					11.33	1	21
HVRalt/7					12.62	1	18
HVRalt/8					13.17	1	18
HVRalt/9					13.51	1	14

HVRalt/10					13.85	1	25
HVR, secondary structure from Huston, et al.[3] (29659– 29852)							
HVRalt/1	194	1018079	25.06	23.99 ± 5.39	0	1	22
HVRalt/2					0.91	1	25
HVRalt/3					3.71	1	15
HVRalt/4					3.78	1	20
HVRalt/5					4.28	1	21
HVRalt/6					6.65	1	17
HVRalt/7					8.27	1	28
HVRalt/8					8.53	1	15
HVRalt/9					8.93	1	19
HVRalt/10					9.72	1	24
3´ UTR BSL extended structure from Huston, et al.[3] (29543–29665; 29846–29876)							
BSLext/1	158	1007602	25.81	24.60 ± 4.94	0	1	27
BSLext/2					1.61	1	15
BSLext/3					4.48	1	24
BSLext/4					6.48	1	21
BSLext/5					7.22	1	15
BSLext/6					7.42	1	17
BSLext/7					7.84	1	18
BSLext/8					8.31	1	19
BSLext/9					9.2	1	17
BSLext/10					9.29	1	16
3´ UTR stem-loop II-like motif, secondary structure based on chemical reactivity from this study (29724–29773)							
S2M/1	50	500000	2.56	5.76 ± 0.57	0	1	25
S2M/2					0.29	2	16
S2M/3					1.46	1	16
S2M/4					1.57	1	13
S2M/5					2.89	1	23
S2M/6					3.04	2	11

S2M/7					3.11	3	22
S2M/8					3.88	1	23
S2M/9					4.02	2	20
S2M/10					4.13	1	21
3´ UTR stem-loop II-like motif, secondary structure using chemical reactivity from Manfredonia, et al.[2] (29724–29773)							
S2M/1	50	500000	2.68	5.86 ± 0.65	0	1	1
S2M/2					1.14	3	1
S2M/3					2.93	1	3
S2M/4					4.6	1	1
S2M/5					5.3	2	2
S2M/6					5.32	1	4
S2M/7					5.51	2	1
S2M/8					5.8	1	1
S2M/9					5.97	2	2
S2M/10					6.38	1	4
3´ UTR stem-loop II-like motif, secondary structure using chemical reactivity from Huston, et al.[3] (29724–29773)							
S2M/1	50	500000	2.74	5.91 ± 0.47	0	1	2
S2M/2					0.19	1	5
S2M/3					0.86	1	1
S2M/4					0.94	1	1
S2M/5					1.2	1	2
S2M/6					1.27	1	3
S2M/7					1.59	1	3
S2M/8					1.61	1	1
S2M/9					1.81	2	2
S2M/10					2.23	1	3

[a]Mean pairwise all-heavy-atom RMSD between 10 lowest energy cluster centers.
[b]Predicted RMSD to true structure.
[c]Rosetta all-atom free energy gap of cluster's lowest energy model compared to lowest energy model discovered in run. REU = Rosetta energy units, calibrated so that 1.0 corresponds approximately to 1 k_BT.
[d]Number of models that appear in each cluster. Clustering was carried out on top 400 models ranked by Rosetta all-atom free energy, based on 5.0 Å threshold, except for small RNAs (SL1-4, SL6-7, s2m), where 2.0 Å threshold was applied.
[e]Number of pockets predicted from fpocket for the cluster center decoy, using default settings for fpocket prediction.

Table S4. FARFAR2-Apo-Riboswitch models, extended data

System/cluster	Length	Models generated	Model convergence (Å)[a]	Predicted minimum RMSD (Å)[b]	E-gap to lowest energy model (REU)[c]	Cluster occupancy[d]	Number of pockets predicted[e]	RMSD to experimental structure with ligand bound
SAM-I riboswitch, RNA-Puzzle 4. PDB ID: 3V7E[11]								
SAM-I/1	126	5768	7.85	10.05 ± 2.55	0	99	17	2.52
SAM-I/2					6.31	6	16	10.76
SAM-I/3					8.03	211	19	8.23
SAM-I/4					18.34	2806	17	9.68
SAM-I/5					25.9	362	16	9.72
SAM-I/6					26.8	22	16	14.83
SAM-I/7					28.76	1	18	17.10
SAM-I/8					29.06	282	15	11.90
SAM-I/9					39.12	140	18	8.07
SAM-I/10					39.77	588	19	11.33
SAM-I/IV riboswitch, RNA-Puzzle 8. PDB ID: 4L81[12]								
SAM-I/IV/1	96	33086	9.76	11.60 ± 2.88	0	4	11	8.83
SAM-I/IV/2					1.77	7	16	11.18
SAM-I/IV/3					2.75	19	16	10.98
SAM-I/IV/4					3.65	15	14	5.23
SAM-I/IV/5					5.16	4	14	9.62
SAM-I/IV/6					5.99	2	14	12.25
SAM-I/IV/7					6.84	1	12	7.69
SAM-I/IV/8					8.78	2	17	7.44
SAM-I/IV/9					9.07	15	14	5.36
SAM-I/IV/10					9.21	1	13	14.13
SAM-IV riboswitch, RNA-Puzzle Unknown Rfam 15. PDB ID: 6UET[13]								
SAM-IV/1	119	10828	8.43	10.52 ± 2.39	0	4	21	7.61
SAM-IV/2					2.16	6	19	3.70
SAM-IV/3					8.44	3	16	6.04

SAM-IV/4					10.13	8	33	11.37
SAM-IV/5					10.15	1	18	9.55
SAM-IV/6					12.88	3	18	7.03
SAM-IV/7					14.4	3	18	8.68
SAM-IV/8					14.72	1	17	8.51
SAM-IV/9					17.51	2	14	8.01
SAM-IV/10					17.94	2	17	6.28
Glycine riboswitch, RNA-Puzzle 3. PDB ID: 3OXE[14]								
Gly/1	84	33442	12.14	13.53 ± 2.13	0	1	9	17.96
Gly/2					1.53	1	10	17.86
Gly/3					3.87	1	12	21.51
Gly/4					7.46	1	12	12.41
Gly/5					7.76	1	13	14.54
Gly/6					7.79	1	10	18.93
Gly/7					8.2	1	11	16.66
Gly/8					10.03	1	13	19.75
Gly/9					10.71	1	12	15.60
Gly/10					10.89	1	9	17.17
Cobalamin riboswitch, RNA-Puzzle 6. PDB ID: 4GXY[15]								
Cobalamin/1	158	28859	14.97	15.81 ± 2.42	0	1	28	20.39
Cobalamin/2					0.47	1	23	13.08
Cobalamin/3					2.41	1	25	24.45
Cobalamin/4					4.14	1	23	19.51
Cobalamin/5					4.84	1	19	17.94
Cobalamin/6					6.1	1	19	24.51
Cobalamin/7					7.48	1	22	19.98
Cobalamin/8					9.07	1	27	25.93
Cobalamin/9					9.74	1	28	19.14
Cobalamin/10					11.56	1	23	16.42
5HT riboswitch, RNA-Puzzle 9. PDB ID: 5KPY[16]								

5HT/1	71	18660	7.89	10.08 ± 2.24	0	44	13	4.56
5HT/2					1.39	27	12	10.12
5HT/3					2.43	32	11	6.97
5HT/4					7.14	12	8	6.54
5HT/5					7.91	32	14	5.29
5HT/6					9.4	9	12	6.99
5HT/7					9.81	16	11	9.59
5HT/8					9.87	10	16	9.37
5HT/9					10	21	9	6.92
5HT/10					10.44	6	12	10.81
ydaO riboswitch, RNA-Puzzle 12. PDB ID: 4QLM[17]								
ydaO/1	117	35506	21.19	20.86 ± 2.43	0	1	23	23.35
ydaO/2					1.66	1	18	16.62
ydaO/3					4.02	1	15	17.26
ydaO/4					5.53	1	20	18.62
ydaO/5					7.2	1	17	14.28
ydaO/6					7.21	1	20	18.13
ydaO/7					7.4	1	13	16.90
ydaO/8					7.75	1	18	13.32
ydaO/9					8.13	1	18	16.23
ydaO/10					9.54	1	15	19.93
ZMP riboswitch, RNA-Puzzle 13. PDB ID: 4XW7[18]								
ZMP/1	60	20297	10.45	12.16 ± 1.94	0	1	4	16.19
ZMP/2					1.07	1	5	10.97
ZMP/3					2.07	1	7	13.30
ZMP/4					2.79	1	7	16.25
ZMP/5					3.88	2	4	11.43
ZMP/6					4.33	3	8	13.83
ZMP/7					6.29	1	7	7.13
ZMP/8					7.26	2	5	14.76
ZMP/9					7.8	1	8	10.62

ZMP/10					8.03	1	6	12.43
Glutamine riboswitch (bound), RNA-Puzzle 14. PDB ID: 5DDP[19]								
Gln (bound)/1	61	24531	11.97	13.39 ± 3.48	0	3	4	10.93
Gln (bound)/2					1.34	2	5	11.71
Gln (bound)/3					1.45	1	4	6.88
Gln (bound)/4					5.31	5	6	11.96
Gln (bound)/5					6.21	2	8	10.85
Gln (bound)/6					7.27	1	7	10.28
Gln (bound)/7					7.78	1	10	16.11
Gln (bound)/8					8.28	8	8	11.33
Gln (bound)/9					9.24	2	6	13.41
Gln (bound)/10					9.64	1	8	10.02
Guanidinium riboswitch, RNA-Puzzle 21. PDB ID: 5NWQ[20]								
Guanidine/1	41	48146	9.26	11.19 ± 1.76	0	21	3	Guanidine/1
Guanidine/2					1.98	10	4	Guanidine/2
Guanidine/3					7.02	62	6	Guanidine/3
Guanidine/4					7.06	24	7	Guanidine/4
Guanidine/5					7.5	11	3	Guanidine/5
Guanidine/6					8.66	48	9	Guanidine/6
Guanidine/7					8.94	10	4	Guanidine/7
Guanidine/8					9.02	16	8	Guanidine/8
Guanidine/9					9.34	19	6	Guanidine/9
Guanidine/10					9.77	6	9	Guanidine/10

[a]Mean pairwise all-heavy-atom RMSD between 10 lowest energy cluster centers.
[b]Predicted RMSD to true structure.
[c]Rosetta all-atom free energy gap of cluster's lowest energy model compared to lowest energy model discovered in run. REU = Rosetta energy units, calibrated so that 1.0 corresponds approximately to 1 k_BT.
[d]Number of models that appear in each cluster. Clustering was carried out on top 400 models ranked by Rosetta all-atom free energy, based on 5.0 Å threshold.
[e]Number of pockets predicted from fpocket for the cluster center decoy, using default settings for fpocket prediction.

Table S5. Primers used in this study.

Name	Purpose	Sequence (5′ to 3′)
Extended 5′ UTR gBlock	DNA template for regions in the extended 5′ UTR	TTCTAATACGACTCACTATTATTAAAGGTTTATACCT TCCCAGGTAACAAACCAACCAACTTTCGATCTCTTGT AGATCTGTTCTCTAAACGAACTTTAAAATCTGTGTGG CTGTCACTCGGCTGCATGCTTAGTGCACTCACGCAGT ATAATTAATAACTAATTACTGTCGTTGACAGGACACG AGTAACTCGTCTATCTTCTGCAGGCTGCTTACGGTTT CGTCCGTGTTGCAGCCGATCATCAGCACATCTAGGTT TCGTCCGGGTGTGACCGAAAGGTAAGATGGAGAGCCT TGTCCCTGGTTTCAACGAGAAAACACACGTCCAACTC AGTTTGCCTGTTTTACAGGTTCGCGACGTGCTCGTAC GTGGCTTTGGAGACTCCGTGGAGGAGGTCTTATCAGA GGCACGTCAACATCTTAAAGATGGCACTTGTGGCTTA GTAGAAGTTGAAAAAGGCGTTTTGCCTCAACTTGAAC AGCCCTATGTGTTCATCAAACGTTCGGATGCTCGAACTG
3′ UTR gBlock	DNA template for regions in the 3′ UTR	TTCTAATACGACTCACTATTTGAAACTCAAGCCTTAC CGCAGAGACAGAAGAAACAGCAAACTGTGACTCTTC TTCCTGCTGCAGATTTGGATGATTTCTCCAAACAATT GCAACAATCCATGAGCAGTGCTGACTCAACTCAGGC CTAAACTCATGCAGACCACACAAGGCAGATGGGCTA TATAAACGTTTTCGCTTTTCCGTTTACGATATATAGTC TACTCTTGTGCAGAATGAATTCTCGTAACTACATAGC ACAAGTAGATGTAGTTAACTTTAATCTCACATAGCAAT CTTTAATCAGTGTGTAACATTAGGGAGGACTTGAAAG AGCCACCACATTTTCACCGAGGCCACGCGGAGTACG ATCGAGTGTACAGTGAACAATGCTAGGGAGAGCTGC CTATATGGAAGAGCCCTAATGTGTAAAATTAATTTTA GTAGTGCTATCCCCATGTGATTTTAATAGCTTCTTAG GAGAATGAC
SL1-4 Forward Primer	PCR amplification for SL1-4 from 5′ UTR gBlock	TTCTAATACGACTCACTATTATTAAAGGTTTATACC
SL1-4 Reverse Primer	PCR amplification for SL1-4 from 5′ UTR gBlock	GTTGTTGTTGTTGTTTCTTTCAGTAATTAGTTATTAATT ATACTGCGTGAGTGC
Reverse complement of SL1-4 Forward Primer	PCR amplification for reverse complement of SL1-4 from 5′ UTR gBlock	TTCTAATACGACTCACTATTCAGTAATTAGTTATTAATT ATACTGCG
Reverse complement of SL1-4 Reverse Primer	PCR amplification for reverse complement of SL1-4 from 5′ UTR gBlock	ATTAAAGGTTTATACCTTCCCAGG
SL2-6_T7_CM-1F	DNA primer for PCR assembly of SL2-6 with 5’ and 3’ flanking “reference hairpins”	TTCTAATACGACTCACTATAGGGTCAGCGAGTAGCTG ACAACGATCTCTTGTAGATCTGTTCTCTAAACGAACTT TAAAATCTGTGTGGC

SL2-6_T7_CM-2R	DNA primer for PCR assembly of SL2-6 with 5' and 3' flanking "reference hairpins"	GCAGCCGAGTGACAGCCACACAGATTT
SL2-6_T7_CM-3F	DNA primer for PCR assembly of SL2-6 with 5' and 3' flanking "reference hairpins"	ACTCGGCTGCATGCTTAGTGCACTCACGCAGTATAAT TAATAACTAATTACTGTCGTTGACAGGACACGAGTAAC TCGTCT
SL2-6_T7_CM-4R	DNA primer for PCR assembly of SL2-6 with 5' and 3' flanking "reference hairpins"	CCCGGACGAAACCTAGATGTGCTGATGATCGGCTGCA ACACGGACGAAACCGTAAGCAGCCTGCAGAAGATAGA CGAGTTACTCGTGTCCT
SL2-6_T7_CM-5F	DNA primer for PCR assembly of SL2-6 with 5' and 3' flanking "reference hairpins"	TTCGTCCGGGTGTGACCGAAAGGTAAGATGGAGAGCC TTGTCCCTGGTTTCAACGAGAAAACACACGTCCAACTC AGTTTGCC
SL2-6_T7_CM-6R	DNA primer for PCR assembly of SL2-6 with 5' and 3' flanking "reference hairpins"	GTTGTTGTTGTTGTTTCTTTGTGTCAGCTACTCGCTGAC TTCACGTCGCGAACCTGTAAAACAGGCAAACTGAGTTGG
Hyper-variable region Forward Primer	PCR amplification for hyper-variable region from 3′ UTR gBlock	TTCTAATACGACTCACTATTCTTTAATCTCACATAGCA ATCTTTAATC
Hyper-variable region Reverse Primer	PCR amplification for hyper-variable region from 3′ UTR gBlock	GTTGTTGTTGTTGTTTCTTTTATTAAAATCACATGGG GATAGCACTAC
FAM-A20-Tail2	RNA extraction and cDNA labeling	/56-FAM/AAAAAAAAAAAAAAAAAAAAGTTGTTGTTGTTTCTTT
RTB000	RT primer for no-modification sample	/56-FAM/AATGATACGGCGACCACCGAGATCTACACTC TTTCCCTACACGACGCTCTTCCGATCTACCAGGCGCT GGGTTGTTGTTGTTGTTTCTTT
RTB001	RT primer for 1M7 modification sample	/56-FAM/AATGATACGGCGACCACCGAGATCTACACTCTTT CCCTACACGACGCTCTTCCGATCTGAGGCCTTGG CCGTTGTTGTTGTTGTTTCTTT
pA-Adapt-Bp	Linker ligated for Illumina sequencing	/5Phos/AGATCGGAAGAGCGGTTCAGCAGGAATGCC GAGACCGATCTCGTATGCCGTCTTCTGCTTG/3Phos/
Eterna Construct 1, ID 9850089	Eterna construct for chemical mapping of genomic positions 45-107	TTCTAATACGACTCACTATAGGAAAGATCTCTTGTAG ATCTGTTCTCTAAACGAACTTTAAAATCTGTGTGGCT GTCACTCGGCTGCAGCAGACGTTCGCGTCTGCAAAA GAAACAACAACAACAAC
Eterna Construct 2, ID 9849692	Eterna construct for chemical mapping of genomic positions 76-136	TTCTAATACGACTCACTATAGGAAATTTTAAAATCTGT GTGGCTGTCACTCGGCTGCATGCTTAGTGCACTCACGCAG TATAATTAAACGTGGGCTTCGGCTCGCGAAAAGAAAC AACAACAACAAC
Eterna Construct 3, ID 9872605	Eterna construct for chemical mapping of genomic positions 172-234	TTCTAATACGACTCACTATAGGAAATCGTCTATCTT CTGCAGGCTGCTTACGGTTTCGTCCGTGTTGCAGC CGATCATCAGCACATCTCCGAAGCTTCGGCTTCG GAAAAGAAACAACAACAACAAC

Eterna Construct 4, ID 9849874	Eterna construct for chemical mapping of genomic positions 172-233	TTCTAATACGACTCACTATAGGAAATCGTCTAT CTTCTGCAGGCTGCTTACGGTTTCGTCCGTG TTGCAGCCGATCATCAGCACATCAGCAGCTGT TCGCAGCTGCAAAAGAAACAACAACAACAAC
Eterna Construct 5, ID 9872974	Eterna construct for chemical mapping of genomic positions 217-277	TTCTAATACGACTCACTATAGGAAACCGATCAT CAGCACATCTAGGTTTCGTCCGGGTGTGACCG AAAGGTAAGATGGAGAGCATTAAGCGGGTCTT CGGGCCTGCAAAAGAAACAACAACAACAAC
Eterna Construct 6, ID 9872770	Eterna construct for chemical mapping of genomic positions 13472-13529	TTCTAATACGACTCACTATAGGAAAGATTTGCGG TGTAAGTGCAGCCCGTCTTACACCGTGCGGCAC AGGCACTAGTACTGATGTAAACGGCGGCTTCGG TCGTTGAAAAGAAACAACAACAACAAC
Eterna Construct 7, ID 9873087	Eterna construct for chemical mapping of genomic positions 29720-29776	TTCTAATACGACTCACTATAGGAAAAGAGACACC ACATTTTCACCGAGGCCACGCGGAGTACGATCG AGTGTACAGTGAACAATGCTACGATACGTTCGC GTATCGAAAAGAAACAACAACAACAAC

Supplemental References

1. Zhang, K.; Zheludev, I. N.; Hagey, R. J.; Wu, M. T.; Haslecker, R.; Hou, Y. J.; Kretsch, R.; Pintilie, G. D.; Rangan, R.; Kladwang, W.; Li, S.; Pham, E. A.; Bernardin-Souibgui, C.; Baric, R. S.; Sheahan, T. P.; V, D. S.; Glenn, J. S.; Chiu, W.; Das, R., Cryo-electron Microscopy and Exploratory Antisense Targeting of the 28-kDa Frameshift Stimulation Element from the SARS-CoV-2 RNA Genome. *bioRxiv* **2020**.
2. Manfredonia, I.; Nithin, C.; Ponce-Salvatierra, A.; Ghosh, P.; Wirecki, T. K.; Marinus, T.; Ogando, N. S.; Snijder, E. J.; van Hemert, M. J.; Bujnicki, J. M.; Incarnato, D., Genome-wide mapping of SARS-CoV-2 RNA structures identifies therapeutically-relevant elements. *Nucleic Acids Res* **2020**.
3. Huston, N. C.; Wan, H.; Araujo Tavares, R. C.; Wilen, C.; Pyle, A. M., Comprehensive in-vivo secondary structure of the SARS-CoV-2 genome reveals novel regulatory motifs and mechanisms. *bioRxiv* **2020**.
4. Lan, T. C. T.; Allan, M. F.; Malsick, L. E.; Khandwala, S.; Nyeo, S. S. Y.; Bathe, M.; Griffiths, A.; Rouskin, S., Structure of the full SARS-CoV-2 RNA genome in infected cells. *bioRxiv* **2020**.
5. Iserman, C.; Roden, C.; Boerneke, M.; Sealfon, R.; McLaughlin, G.; Jungreis, I.; Park, C.; Boppana, A.; Fritch, E.; Hou, Y. J.; Theesfeld, C.; Troyanskaya, O. G.; Baric, R. S.; Sheahan, T. P.; Weeks, K.; Gladfelter, A. S., Specific viral RNA drives the SARS CoV-2 nucleocapsid to phase separate. *Mol. Cell, in press* **2020**.
6. Rangan, R.; Zheludev, I. N.; Das, R., RNA genome conservation and secondary structure in SARS-CoV-2 and SARS-related viruses. *bioRxiv* **2020**.
7. Sun, L.; Li, P.; Ju, X.; Rao, J.; Huang, W.; Zhang, S.; Xiong, T.; Xu, K.; Zhou, X.; Ren, L.; Ding, Q.; Wang, J.; Zhang, Q. C., In vivo structural characterization of the whole SARS-CoV-2 RNA genome identifies host cell target proteins vulnerable to re-purposed drugs. *bioRxiv* **2020**.
8. Kelly, J. A.; Dinman, J. D., Structural and functional conservation of the programmed -1 ribosomal frameshift signal of SARS-CoV-2. *bioRxiv* **2020**.
9. Wacker, A.; Weigand, J. E.; Akabayov, S. R.; Altincekic, N.; Bains, J. K.; Banijamali, E.; Binas, O.; Castillo-Martinez, J.; Cetiner, E.; Ceylan, B.; Chiu, L. Y.; Davila-Calderon, J.; Dhamotharan, K.; Duchardt-Ferner, E.; Ferner, J.; Frydman, L.; Furtig, B.; Gallego, J.; Grun, J. T.; Hacker, C.; Haddad, C.; Hahnke, M.; Hengesbach, M.; Hiller, F.; Hohmann, K. F.; Hymon, D.; de Jesus, V.; Jonker, H.; Keller, H.; Knezic, B.; Landgraf, T.; Lohr, F.; Luo, L.; Mertinkus, K. R.; Muhs, C.; Novakovic, M.; Oxenfarth, A.; Palomino-Schatzlein, M.; Petzold, K.; Peter, S. A.; Pyper, D. J.; Qureshi, N. S.; Riad, M.; Richter, C.; Saxena, K.; Schamber, T.; Scherf, T.; Schlagnitweit, J.; Schlundt, A.; Schnieders, R.; Schwalbe, H.; Simba-Lahuasi, A.; Sreeramulu, S.; Stirnal, E.; Sudakov, A.; Tants, J. N.; Tolbert, B. S.; Vogele, J.; Weiss, L.; Wirmer-Bartoschek, J.; Wirtz Martin, M. A.; Wohnert, J.; Zetzsche, H., Secondary structure determination of conserved SARS-CoV-2 RNA elements by NMR spectroscopy. *Nucleic Acids Res* **2020**.
10. Robertson, M. P.; Igel, H.; Baertsch, R.; Haussler, D.; Ares, M., Jr.; Scott, W. G., The structure of a rigorously conserved RNA element within the SARS virus genome. *PLoS Biol.* **2005,** *3* (1), e5.
11. Baird, N. J.; Zhang, J.; Hamma, T.; Ferre-D'Amare, A. R., YbxF and YlxQ are bacterial homologs of L7Ae and bind K-turns but not K-loops. *RNA* **2012,** *18* (4), 759-70.

12. Trausch, J. J.; Xu, Z.; Edwards, A. L.; Reyes, F. E.; Ross, P. E.; Knight, R.; Batey, R. T., Structural basis for diversity in the SAM clan of riboswitches. *Proc Natl Acad Sci U S A* **2014,** *111* (18), 6624-9.
13. Zhang, K.; Li, S.; Kappel, K.; Pintilie, G.; Su, Z.; Mou, T. C.; Schmid, M. F.; Das, R.; Chiu, W., Cryo-EM structure of a 40 kDa SAM-IV riboswitch RNA at 3.7 A resolution. *Nat Commun* **2019,** *10* (1), 5511.
14. Huang, L.; Serganov, A.; Patel, D. J., Structural insights into ligand recognition by a sensing domain of the cooperative glycine riboswitch. *Mol Cell* **2010,** *40* (5), 774-86.
15. Peselis, A.; Serganov, A., Structural insights into ligand binding and gene expression control by an adenosylcobalamin riboswitch. *Nat Struct Mol Biol* **2012,** *19* (11), 1182-4.
16. Porter, E. B.; Polaski, J. T.; Morck, M. M.; Batey, R. T., Recurrent RNA motifs as scaffolds for genetically encodable small-molecule biosensors. *Nat Chem Biol* **2017,** *13* (3), 295-301.
17. Ren, A.; Patel, D. J., c-di-AMP binds the ydaO riboswitch in two pseudo-symmetry-related pockets. *Nat Chem Biol* **2014,** *10* (9), 780-6.
18. Trausch, J. J.; Marcano-Velazquez, J. G.; Matyjasik, M. M.; Batey, R. T., Metal Ion-Mediated Nucleobase Recognition by the ZTP Riboswitch. *Chem Biol* **2015,** *22* (7), 829-37.
19. Ren, A.; Xue, Y.; Peselis, A.; Serganov, A.; Al-Hashimi, H. M.; Patel, D. J., Structural and Dynamic Basis for Low-Affinity, High-Selectivity Binding of L-Glutamine by the Glutamine Riboswitch. *Cell Rep* **2015,** *13* (9), 1800-13.
20. Huang, L.; Wang, J.; Wilson, T. J.; Lilley, D. M. J., Structure of the Guanidine III Riboswitch. *Cell Chem Biol* **2017,** *24* (11), 1407-1415 e2.